Polymorphic stability of AlAs/GaAs superlattices at high pressure

L. J. Cui,* U. D. Venkateswaran,† and B. A. Weinstein
Department of Physics, 239 Fronczak Hall, SUNY at Buffalo, Buffalo, New York 14260

F. A. Chambers
Amoco Technology Co., P.O. Box 3011, Naperville, Illinois 60566
(Received 24 May 1991)

The pressure-induced α-β structural transitions in [001]-oriented AlAs/GaAs superlattices (SL's) are studied by Raman scattering using a 300-K diamond-anvil press. The threshold pressures of the forward and reverse transitions in the AlAs and GaAs constituents of each SL are accurately measured for layer thicknesses in the range 300–20 Å, and comparison is made to the bulk transitions reported in the preceding paper. We obtain direct microscopic evidence that (i) the SL constituents transform separately (first AlAs, then GaAs) or simultaneously, depending on whether the *AlAs layers* are thicker or thinner than ~50 Å; (ii) overpressing of zinc-blende AlAs by ~5 GPa above its bulk stability limit is *not* matched by GaAs underpressing: (iii) the postreversal condition of the SL's is marked by increasing signs of bulk and interface disorder as the constituent layer thickness decreases. The AlAs overpressing shows that the effective polymorphic stability of these SL's is GaAs controlled over a wide layer-thickness range. The thermodynamics of high-pressure SL transitions is discussed. We find that the β-AlAs/α-GaAs sixfold-fourfold interface encountered at high pressure has the empirical energy density $\sigma^{\beta\alpha}=0.12\pm0.02$ eV/Å^2, and is best described by a disordered-interface model. Comparison to microscopic theory for a *pseudomorphic* sixfold-fourfold interface shows that the calculated geometry probably does not occur at the static interfaces of AlAs/GaAs SL's, but might exist during transformation at the kinetic boundary of small β nuclei forming within an α matrix. Alloylike pressure stability is predicted when the SL periods are substantially thinner than the smallest β nuclei.

I. INTRODUCTION

Virtually all past work on pressure-induced phase transitions in semiconductors, experiment[1–3] and theory,[4–6] has dealt with bulk homogeneous solids, for which the surfaces were assumed to be relaxed at infinity, and there were no internal interfaces. There has, however, been growing interest in the influence of interface boundary constraints on the nature and threshold of these transitions.[7–10] Over the last two decades progress in epitaxial growth has made possible heterogeneous crystalline systems[11,12] in which constraints due to interface bonding can strongly influence, and for very thin layers, perhaps even dominate, stability and other properties.[13–16] Hence there is a clear need to explore the extent that heteroepitaxy modifies the high-pressure stability of semiconductor polymorphs, and this is the underlying physical issue addressed here. The α-β transformations in *bulk* AlAs and GaAs were discussed fully in the preceding paper (Paper I). The present account (Paper II) describes detailed Raman and parallel visual experiments on the analogous pressure-induced transitions in AlAs/GaAs superlattices (SL's), attempting to understand their novel features in terms of heterointerface energetics.

Some examples involving epitaxial growth at standard pressure (P) of semiconductors, or of metals on semiconductor substrates, illustrate the importance of heterointerface effects for polymorphic stability. Metastable films of bcc Co (the stable bulk phase is hcp) can be deposited on [110]-oriented GaAs substrates using molecular-beam epitaxy (MBE).[17] Thin layers of zinc-blende (ZB) MnSe (the stable bulk phase is rocksalt B1) can be grown by MBE within MnSe/ZnSe SL's; to achieve this, the interface bonding must accommodate a large misfit strain, ~4.7%.[18] A similar case is the epitaxial stabilization of ZB $Zn_{1-x}Fe_xSe$ on GaAs for $0.22\leq x\leq 1$, but here smaller misfit strains allow substantially thicker films.[19] Lastly, films of α(ZB)-Sn grown on InSb or CdTe substrates can be stabilized against heating (1 bar) by as much as 102° above the normal bulk transition at 286.2 K to the β-Sn phase;[20] the stabilization decreases with increasing film thickness, resembling the overpressing phenomena discussed below for AlAs/GaAs SL's.

The earlier visual experiments on high-pressure phase changes in AlAs/GaAs SL's (Ref. 7) revealed several layer-thickness dependent effects not present in bulk semiconductors. In particular, the ZB phase of thin AlAs layers can be overpressed[21] far above the bulk AlAs α-β transition, ultimately by some 5 GPa to the α-β threshold of bulk GaAs. Furthermore, depending on the layer thickness, each SL constituent, and even individual layers, can transform separately—first the AlAs layers at P_1^t and then the GaAs layers at P_2^t. (This notation for the forward α-β thresholds is employed throughout; as in Paper I, $P_a^t=12.4$ GPa and $P_g^t=17.3$ GPa denote the α-β thresholds of bulk AlAs and GaAs, respectively, and R^t signifies a reverse transition.) The actual sequence of phase changes for one of the superlattice samples studied here is chronicled by the photomicrographs in Fig. 1; the color and black and white plates in Refs. 7 and 22 show

additional examples. The extent of AlAs overpressing is apparent in these photographs from the higher onset pressures for opacity in the SL's compared to P_a^t. The occurrence of transitions in individual AlAs layers was deduced (see Ref. 7) from *constant-pressure* observations of progressive specimen darkening by sudden *discrete steps*. Independent confirmation of AlAs overpressing has been reported for short period AlAs/GaAs SL's.[23] Also similar-size CdTe/ZnTe SL's exhibit CdTe overpressing,[24] although no evidence for separate CdTe and ZnTe transitions was found for this strained-layer system.

The Raman studies described here provide precise microscopic confirmation of the earlier findings in AlAs/GaAs SL's, and extend these findings to a larger subset of SL's having different AlAs and GaAs layer thicknesses. In addition, focusing on issues raised by Refs. 7–9, the present SL experiments determine the threshold pressures P_2^t for the α-β transition of the GaAs layers, establish the reverse nature [i.e., $\beta \rightarrow$ZB(α)] of the decreasing-pressure transitions at R^t, and reveal substantial changes in heterointerface quality produced by the transformations. These results bear importantly on our analysis of the phase changes occurring within SL layers compared to their bulk counterparts.

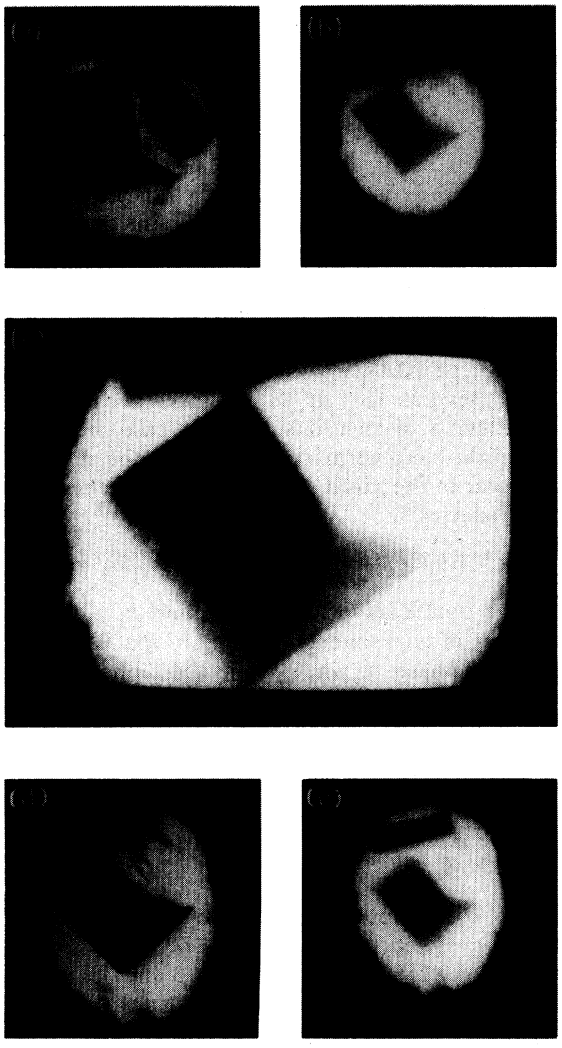

FIG. 1. Photomicrographs showing free-standing specimens of SL2 (GaAs/AlAs 225 Å/75 Å, see Table I) undergoing high-pressure phase transitions in the DAC. (a) 0.3 GPa. Initial state of sample is visibly opaque. (b) 10.5 GPa. Band gap has increased to ~2.3 eV. (c) 14.6 GPa at AlAs transition. Sample is held in partly transformed state—opaque region contains β-AlAs/α-GaAs. (d) 16.5 GPa. AlAs transition is complete; GaAs is still in ZB (α) phase. (e) 8.5 GPa on first cycle down of pressure. Most [~90%, note cloudiness compared to (b)] of β-AlAs has reversed to ZB phase; see text. Frames were digitized from color super-VHS tape for processing and printing.

To understand the differences between SL and bulk transitions, we are led (as in Paper I) to consider the energetics of the α/β interface. However, in SL's this boundary is a *static* planar heterointerface, instead of the *momentary* homointerface treated for bulk semiconductors. The success of dislocation-strain theory for describing epitaxial growth of mismatched solids[13,14,25] suggests that a macroscopic viewpoint might be fruitful for treating the α/β interface energetics, and this is the approach we follow. Martin[8] has reported density-functional calculations for some model α/β interfaces under pressure. It seems clear from this, and recent microscopic treatments of SL stability at ambient pressure,[26] that additional work using modern total-energy methods is desirable to investigate the high-pressure phases of SL's. A significant outcome of our study is an empirical value for the α/β interface energy that compares favorably with the earlier microscopic results.[7,8]

In Sec. II we describe a macroscopic theory of pressure-induced SL transitions, first formulating the thermodynamics to include general interface terms, and then applying the dislocation-strain picture to the specific problem of transitions in AlAs/GaAs SL's. Section III discusses measurement procedures which were required for the SL's, and not given in Paper I. A comprehensive account of our Raman results follows in Sec. IV. This includes subsections dealing with the following: (Sec. IV A) the evidence in SL's for separate versus simultaneous GaAs and AlAs transitions depending on layer thickness, (Sec. IV B) the related occurrence of AlAs overpressing without GaAs underpressing, (Sec. IV C) the β-α reverse transitions in SL's, and (Sec. IV D) the transition-induced degradation of the SL heterointerfaces. Section V discusses these results using the formalism developed in Sec. II; we focus on the validity of three limiting pictures—the full equilibration, the disordered-interface, and the equivalent alloy pictures. Comparisons to relevant microscopic calculations are made where possible. Concluding remarks relating the findings in both companion papers and outlining connections to epitaxial growth are presented in Sec. VI.

II. MACROSCOPIC THEORY OF PRESSURE-INDUCED SL TRANSITIONS

It is well known that successful epitaxial growth of lattice-mismatched materials hinges on the energy competition between strain and misfit dislocations at internal heterointerfaces.[13,14,25] This concept has also been used

to investigate the growth and stability of metastable heterostructures under ambient conditions.[27] Here we present a theory of SL phase stability under applied hydrostatic pressure that is based on similar considerations. The case of initially lattice-matched constituents, appropriate to AlAs/GaAs, is considered in detail, but the formalism is sufficiently general to include 1 atm mismatch. Although our approach is inherently macroscopic, we shall see that it provides an excellent framework for understanding many of the observations in Sec. IV, and for interpreting comparisons with microscopic theory. A preliminary account of the present treatment is given in Ref. 9.

Consider a SL composed of two semiconductors labeled a and g, each of which can exist in two structural phases α and β, with α being the $P=0$ (1 bar) ZB phase and β being the high-pressure phase. The total Gibbs free energy of the SL when, for example, material a is in the β phase and material g is in the α phase is denoted by

$$G_{ag}^{\beta\alpha}=U_{ag}^{\beta\alpha}+PV_{ag}^{\beta\alpha}-TS_{ag}^{\beta\alpha} . \tag{1}$$

Here the quadruple-indexed quantities U, V, and S refer, respectively, to the internal energy, volume, and entropy of the entire SL; note that corresponding phase and material indices are vertically aligned. It is reasonable to express the SL internal energy as a linear sum of bulk and interface terms. The usual condition $G_{ag}^{\alpha\alpha}(P_1^t)=G_{ag}^{\beta\alpha}(P_1^t)$ determines the $\alpha/\alpha\rightarrow\beta/\alpha$ phase threshold at P_1^t. This leads to

$$(U_a^\beta-U_a^\alpha)+(U^{\beta\alpha}-U^{\alpha\alpha})=-P_1^t(V_{ag}^{\beta\alpha}-V_{ag}^{\alpha\alpha}) +T(S_{ag}^{\beta\alpha}-S_{ag}^{\alpha\alpha}) , \tag{2}$$

where the first and second left-hand parentheses contain bulk contributions for material a and interface contributions, respectively. Bulk energies for material g cancel because g has not transformed.

The first simplification one would like to make involves neglecting the entropy term. Thermal data on the analogous α-β transitions in bulk semiconductors show that the phase-boundary slopes $(dP/dT)_{\beta\alpha}$ are typically rather small, e.g., $\sim -1/600$ GPa/K for InSb (Ref. 28) and $\sim -1/200$ GPa/K for Ge.[29] Using Clapeyron's equation, one finds the entropy contributions to be ~ 15–20% of the total internal-energy change. This should continue to hold for our 300-K SL transformations, since the temperature is not high enough to cause substantial interfacial diffusion during the transitions. Hence, at the present level of treatment entropy contributions can safely be neglected.

Another valid approximation concerns the bulk α-β energy difference. At the threshold P_a^t of material a in isolation one has $U_a^\beta-U_a^\alpha=-P_a^t(V_a^\beta-V_a^\alpha)$, where V_a^β and V_a^α are bulk volumes corresponding to the amount of material a present in the SL. At $P_1^t\neq P_a^t$ it is straightforward to show in the harmonic approximation that

$$U_a^\beta-U_a^\alpha\simeq -P_a^t(V_a^\beta-V_a^\alpha) +P_a^t(P_1^t-P_a^t)\left\{\left[\frac{\partial^2U_a^\beta}{\partial V^2}\right]^{-1}-\left[\frac{\partial^2U_a^\alpha}{\partial V^2}\right]^{-1}\right\} . \tag{3}$$

The second right-hand term can be neglected for $(P_1^t-P_a^t)$ much smaller than the bulk modulus of material a.[30] This is well obeyed for the 5 GPa maximum observed overpressing in AlAs/GaAs SL's.

Additionally, consider the relation between the total volume change of the SL when only its a component transforms, and the volume change for the transition of the equivalent amount of material a in *bulk form*, viz., the relation between $(V_{ag}^{\beta\alpha}-V_{ag}^{\alpha\alpha})$ and $(V_a^\beta-V_a^\alpha)$. For the cubic→cubic or cubic→tetragonal changes common in bulk semiconductors (see Paper I, Sec. I), conventional linear-strain theory[31] gives at P_1^t

$$(V_{ag}^{\beta\alpha}-V_{ag}^{\alpha\alpha})=(V_a^\beta-V_a^\alpha) +2\left[\frac{1-2\nu}{1-\nu}\right](V_a^\beta\delta_a^{\beta\alpha}+V_g^\alpha\delta_g^{\alpha\beta} -V_a^\alpha\epsilon_a^{\alpha\alpha}-V_g^\alpha\epsilon_g^{\alpha\alpha}) , \tag{4}$$

where ν (~ 0.3) is Poisson's ratio. In Eq. (4) the ϵ's represent the planar misfit-induced strains that develop in components a and g when they are mated together at P_1^t in their α phases, and the δ's are the analogous strains for the β phase of a mated (again at P_1^t) with the α phase of g. Of course, these strains can be small in the absence of misfit (e.g., in AlAs/GaAs the ϵ's are ~ 0, but the δ's could be several %), or in the presence of sufficient strain-relieving dislocations. In any case, however, the second right-hand term of Eq. (4) can be neglected to terms linear in the misfit strains because mechanical equilibrium requires[25,32]

$$h_a^{\alpha\alpha}\epsilon_a^{\alpha\alpha}+h_g^{\alpha\alpha}\epsilon_g^{\alpha\alpha}\approx 0 \quad\text{and}\quad h_a^{\beta\alpha}\delta_a^{\beta\alpha}+h_g^{\alpha\beta}\delta_g^{\alpha\beta}\approx 0 \tag{5}$$

where the double-superscripted h_a and h_g are the layer thicknesses of components a and g *in the SL* when both are in the α phase, or when a is in the β phase and g is in the α phase.

Combining Eqs. (2)–(4) under the above approximations, one arrives at the following simple expression for the α-phase overpressing of material a:

$$-\frac{2(\sigma^{\beta\alpha}-\sigma^{\alpha\alpha})}{(\Delta V/V)^{\beta\alpha}h_a^{\alpha\alpha}}=P_1^t-P_a^t . \tag{6}$$

Here the σ's denote the interface-energy densities per unit SL area corresponding to $U^{\beta\alpha}$ and $U^{\alpha\alpha}$, and $(\Delta V/V)^{\beta\alpha}\sim -15\%$ to -20% (Refs. 3 and 33) is the fractional volume change during a *bulk* transition (taken to be the same for both materials here). Analogous reasoning shows that the β phase of material g should be *underpressed* in a SL according to

$$\frac{2(\sigma^{\beta\beta}-\sigma^{\beta\alpha})}{(\Delta V/V)^{\beta\alpha}h_g^{\alpha\beta}}=P_g^t-P_2^t . \tag{7}$$

These expressions explicitly relate modifications in the phase stability of SL's compared with their bulk constituents to differences in heterointerface energy density. Note the inverse dependence on the *transformed constituent's* layer thickness. The error introduced by using the linear-strain approximation should not exceed

$(\Delta V/V)^{\beta\alpha}$, which is of the same order as the neglected entropy changes. Hence we expect the accuracy of Eqs. (6) and (7) to be $\sim 15-20\%$.

To go further, the interface energy densities must be calculated for the α/α, β/α, and β/β SL phases. The most direct course would be to perform microscopic total-energy calculations subject to the appropriate heterointerface constraints. This approach has been employed for a pseudomorphic [111]-oriented fourfold-sixfold interface[8] (see Sec. V below), and for various adamantine structure fourfold-fourfold combinations at $P=0$.[26] Instead, we shall model the heterointerface energetics by means of the same macroscopic strain-dislocation approach commonly used to describe the epitaxial growth of mismatched semiconductors. In the present problem, however, the mismatch results from a phase transition instead of (or, for strained-layer SL's, in addition to) from growth. This macroscopic viewpoint is expected to have validity as long as the layers do not become atomically thin.

According to the conventional picture, the extra energy arising from an interface between two mismatched lattices contains two contributions—one due to the strain field of misfit dislocations, and the other due to the homogeneous misfit strain.[13,14,25] For a SL with fractional misfit f between its bulk constituents, the energy per unit area from these two terms is given, respectively, by[14]

$$\sigma_d=\frac{2}{\lambda_d}\left\{\frac{\mu b^2}{4\pi(1-\nu)}\left[\ln\left[\frac{\sqrt{h_a h_g}}{b}\right]+C\right]\right\}, \tag{8}$$

$$\sigma_s=\mu\left[\frac{1+\nu}{1-\nu}\right]\frac{h_a h_g}{h_a+h_g}\xi^2, \tag{9}$$

per interface. In these equations elastic isotropy is assumed. μ and ν are the shear modulus and Poisson's ratio taken to be equal in both materials, b is the Burger's displacement, λ_d the linear distance between misfit dislocations, ξ the relative elastic strain between the two materials, C a constant due to the dislocation core, and, as before, h_a and h_g denote the SL layer thicknesses. Here we shall consider explicitly only orthogonal noninteracting edge dislocations, with $\xi\le f$ and $\lambda_d=b/(f-\xi)$. The Eq. (8) expression in curly brackets is the energy per unit length of a single dislocation. The expression for a general dislocation is similar except for a geometrical factor of order unity.[25,34] Minimizing the sum $\sigma_d+\sigma_s$ with respect to ξ gives the equilibrium strain ξ^* as

$$\xi^*=\frac{b}{4\pi(1+\nu)}\frac{h_a+h_g}{h_a h_g}\left[\ln\left[\frac{\sqrt{h_a h_g}}{b}\right]+C\right]. \tag{10}$$

The equality $\xi^*=f$ defines the critical condition for infinite separation of dislocations, which is often applied to pseudomorphic growth of strained-layer SL's (SLSL's).[14]

Returning to the specific phase-transition problem at hand, one expects that $\sigma^{\alpha\alpha}$ in Eq. (6) is small for the lattice-matched α-AlAs/α-GaAs system, since $\xi^*\simeq 0$, and (ideally) there should be very few dislocations. (However, this would not be true for SLSL's.[24,35]) If, as we shall assume, AlAs and GaAs undergo the same structural change and volume decrease, $\sigma^{\beta\beta}$ should likewise be small on the condition that the transformed interfaces can fully equilibrate. In comparison, $\sigma^{\beta\alpha}$ should be substantial because the volume change $(\Delta V/V)^{\beta\alpha}$ $\sim -15\%$ to -20% ensures that there will be a large misfit between β-AlAs and α-GaAs, and this will enable both dislocation and strain terms to contribute. For the ZB$\rightarrow$B1(rocksalt) transformation thought to be prototypical in AlAs,[8,36] let us introduce the *transition* misfit q referred to the bulk lattice constants at P_1^t,

$$q=\frac{a_a^\beta-a_g^\alpha}{a_g^\alpha}. \tag{11}$$

Since the case of interest involves a cubic$\rightarrow$cubic change, and the α/α-phase is virtually lattice matched, we expect for AlAs/GaAs that $q\approx(1/3)(\Delta V/V)^{\beta\alpha}$. (For a SLSL, there would be an additive correction due to the α/α-phase misfit.) Again, on the condition of *full equilibration* of the β-AlAs/α-GaAs interface, $\sigma^{\beta\alpha}$ in Eq. (6) should be given by the sum of Eqs. (8) and (9) evaluated at ξ^*, with $|q|$ substituted for f in the dislocation separation, i.e., $\lambda_d^{\beta\alpha}=b/(|q|-\xi^*)$.

Considering now the second SL transformation involving the GaAs layers (viz., material g), one expects the dislocation configuration of the β/α interface to be the same at P_2^t as at P_1^t. The condition $\sigma^{\beta\alpha}(P_1^t)\simeq\sigma^{\beta\alpha}(P_2^t)$ should then be satisfied, save for small elastic terms, which we neglect. It follows from Eqs. (6) and (7), assuming *full equilibration* allows $\sigma^{\beta\beta}\approx\sigma^{\alpha\alpha}\approx 0$, that the overpressing of ZB AlAs implies a complementary underpressing of the β-phase of GaAs according to the relation

$$P_g^t-P_2^t\approx\frac{h_a^{\alpha\alpha}}{h_g^{\alpha\beta}}(P_1^t-P_a^t). \tag{12}$$

The predicted behavior of this full-equilibration (FE) limit is illustrated by the solid curves in Fig. 2 for the transitions in AlAs/GaAs SL's with $h_a^{\alpha\alpha}=h_g^{\alpha\alpha}$; for simplicity, we use the as-grown layer thicknesses in Fig. 2 and suppress the correction of order q between $h_g^{\alpha\alpha}$ and $h_g^{\alpha\beta}$. The complementarity between AlAs overpressing and GaAs underpressing is apparent. The region between the two horizontal portions of the curves for layer thicknesses below 40 Å corresponds to a pseudomorphic β-AlAs/α-GaAs SLSL with $\xi^*=|q|$ and no dislocations. This is the continuum limit of the configuration Martin has treated microscopically.[8]

An alternative to the full-equilibration limit is the disordered-interface (DI) limit, in which the $\alpha/\alpha\rightarrow\beta/\alpha$ transition creates such a dense packing of interface dislocations that the interface cannot reorder itself during the subsequent $\beta/\alpha\rightarrow\beta/\beta$ transition. In that case Eq. (12) is not applicable. The interface energies $\sigma^{\beta\alpha}$ and $\sigma^{\beta\beta}$ become dominated by dislocations with negligible homogeneous strain, and, if the temperature is too low for the disorder to anneal (likely at 300 K), the dislocation densities for both the β/α and β/β interfaces should be similar. This leads to $\sigma^{\beta\beta}\approx\sigma^{\beta\alpha}$, and by Eq. (7) there should be *no* underpressing of the β-GaAs phase regardless of the layer thicknesses or their ratios. Of course, it remains

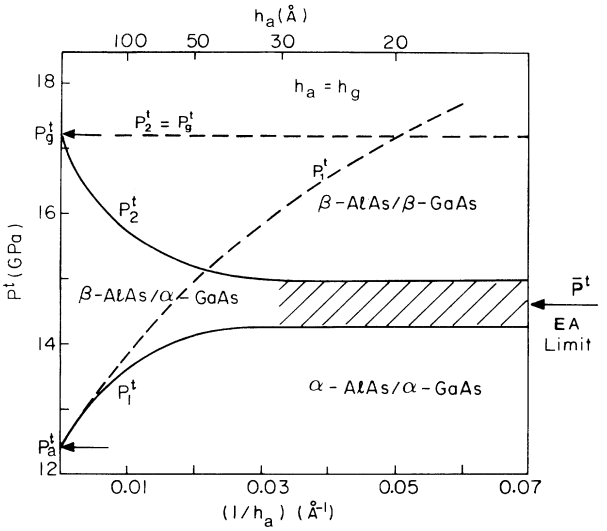

FIG. 2. Calculated "phase diagram" for GaAs/AlAs SL's with equal as-grown layer widths, h_a (AlAs) and h_g (GaAs), showing various α-β thresholds P^t as a function of $1/h_a$. Solid and dashed curves describe P_1^t and P_2^t in the full-equilibration (FE) and disordered-interface (DI) limits, respectively. Arrows give the bulk AlAs and GaAs thresholds, and the equivalent alloy (EA) average. The α/α, β/α, and β/β stability regions predicted by the FE limit are labeled; cross hatched area corresponds to a pseudomorphic β-AlAs/α-GaAs FE geometry. Calculations are performed for ZB→B1 lattice change with 5% decrease in cubic a_0.

true that $\sigma^{\alpha\alpha}\sim 0$ in AlAs/GaAs SL's, so that ZB-AlAs overpressing still occurs. The latter again can be calculated from Eq. (6), but now by including only dislocation contributions—viz., $\sigma^{\beta\alpha}$ should be given by Eq. (8) with $\lambda_d \approx b/|q|$. The dashed curves in Fig. 2 show the predictions of the DI limit for the ZB→B1 transition with $q\sim -5\%$. The overpressing of ZB AlAs does not saturate as before, but continues to increase as the AlAs layers become thinner until $P_1^t = P_2^t = P_g^t$; in contrast, for all layer thicknesses $P_2^t = P_g^t$. There are, at present, no microscopic calculations for this rather complicated limit.

A final case to consider is the equivalent alloy (EA) limit. It is physically clear that as the layers in a SL approach atomic dimensions, the SL stability should approach that of an equivalent homogeneous alloy with the same mole fractions of each constituent. One then expects the SL to undergo the $\alpha/\alpha \rightarrow \beta/\beta$ transition monolithically, without ever entering the β/α configuration. Hence, the interface energy $U^{\beta\alpha}$ is not relevant, and, assuming both constituents have the same bulk transition (preserving lattice matching), $U^{\beta\beta}$ and $U^{\alpha\alpha}$ should have similar small magnitudes. It is easy to show that the condition of equal Gibbs energies at the phase boundary now gives, to terms linear in strain,

$$\bar{P}^t = \frac{h_a^{\alpha\alpha} P_a^t + h_g^{\alpha\alpha} P_g^t}{h_a^{\alpha\alpha} + h_g^{\alpha\alpha}} , \tag{13}$$

where $\bar{P}^t$ is the $\alpha/\alpha \rightarrow \beta/\beta$ threshold, and entropy changes are again disregarded. Equation (13) exhibits the expected alloylike behavior with respect to the mole fractions of each constituent.

Let us inquire into the conditions of validity for the EA limit. To do this, one should consider the nucleation mechanism by which the first-order α-β transition proceeds.[28] The importance of nucleation is illustrated by Fig. 3 within the context of the following discussion. Referring to Eq. (2) of Paper I, the minimum nucleation radius for β nuclei to grow within the α phase of a single substance is related to the homointerface energy density $\sigma_0^{\beta\alpha}$ and the forward-reverse threshold hysteresis. When the minimum nucleation size is much less than the layer thickness of a SL constituent, the β phase can nucleate and grow within this constituent [as in Fig. 3(a) for material a] much as for a bulk transition. The threshold is modified by the additional energy of the infinite planar heterointerfaces, but otherwise growth proceeds without involving material g, except for thin disordered regions where β nuclei overlap the heterointerfaces. This picture breaks down when [as in Fig. 3(b)] the SL period is smaller than the minimum nucleation radius. In that limit, β nuclei must encompass both constituents in approximate proportion to their layer thicknesses. Since entropy changes during the transition are not significant for the temperatures of interest, the situation should be analogous to a bulk alloy transformation [as depicted in Fig. 3(c)] with the SL threshold given by Eq. (13).

For SL systems such as AlAs/GaAs, composed of chemically similar constituents, it seems reasonable that the heterointerface energy density $\sigma^{\beta\alpha}$ in Eqs. (6) and (7) will be similar in magnitude to $\sigma_0^{\beta\alpha}$. In Sec. V, this hy-

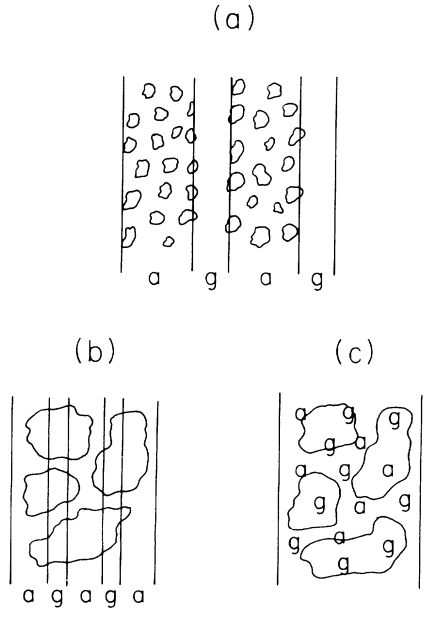

FIG. 3. Pressure-induced β-phase nucleation within the α phase of ordered and disordered heterogeneous solids. (a) Layer thickness greatly exceeds the minimum nucleation size. (b) Minimum nucleation size is much greater than the layer thickness so that β-phase growth involves both a and g, much as in (c) for a disordered alloy.

pothesis is used to estimate the onset of the EA limit based on our AlAs overpressing data.

III. EXPERIMENT

Many aspects of the Raman-scattering system, the high-pressure diamond-anvil-cell (DAC) apparatus, and the experimental procedures are the same in the present work on AlAs/GaAs SL's, as discussed previously for bulk films in Paper I. Hence, we concentrate here on details unique and important to the SL experiments, referring the reader to Paper I for experimental factors common to both studies.

Six different GaAs/AlAs SL's, designated SL1–SL6, with periods in the range 450-70 Å, will be discussed. Their architectures and methods of growth are given in Table I. The SL samples were grown by either molecular-beam epitaxy or organometallic chemical vapor deposition (OMCVD) on GaAs substrates with [001] orientation. Details of the growth and characterization of these high-equality SL's are discussed elsewhere.[37,38] The low-frequency Raman spectra presented in Fig. 4 for SL4 grown by MBE and for SL6 grown by OMCVD further illustrate the quality of growth in the two cases. Folded-mode doublets up to fourth order are observed for both samples, indicating excellent superperiodicity, equally well defined for each growth method.[39]

For all but one of our SL measurements, the GaAs substrates were removed from the samples by selective etching in order to exclude any substrate related phenomena. The etchant was 30% H_2O_2 made slightly basic (pH of 7.3±0.2) by adding NH_4OH.[40] After chemically polishing the substrate to ~20 μm thickness as in Paper I, the specimen is immersed in the GaAs selective etch, which is continuously agitated to remove the surface oxide layers that form during etching. The etching rate is ~10 μm/h. When the process is complete, the specimen is gently floated out of the etchant and thoroughly rinsed with cold distilled water. As indicated by the layer dimensions in Table I, the resulting free-standing SL samples range in thickness from 0.7 to 2.7 μm. After the substrate is removed, the surface underneath appears just as brilliant as the original front epitaxial surface when examined under a standard optical microscope. Extensive pretransition measurements for $P < P_1^t$ show little difference between the Raman spectra of free-standing

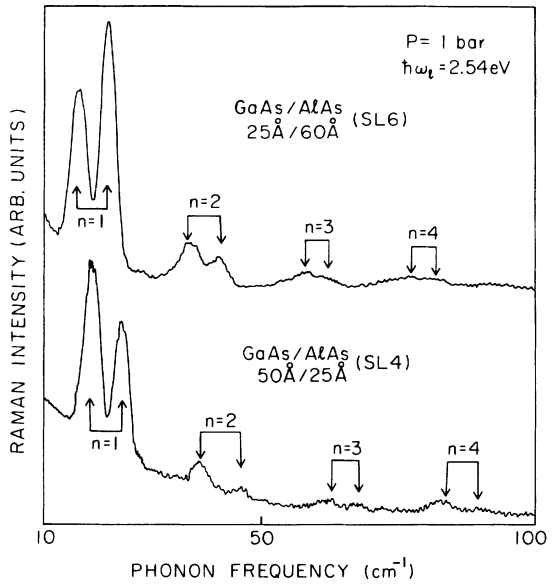

FIG. 4. Characterization at 1 bar of SL4 and SL6 grown by MBE and OMCVD, respectively, reflecting high film quality via the presence of well-defined zone-folded modes.

SL's prepared in this way and those of the corresponding substrated specimens.[41] For one loading of SL4, we purposely retained the ~20 μm substrate to check whether the transition threshold would differ from that observed in the same free-standing SL. (See Sec. IV A.)

The DAC loading procedure for free-standing SL's is more difficult to execute than for bulk samples (Paper I). Residual electrostatic charges on the specimens, diamonds, and gasket often cause the thin SL specimens to "fly" away from the gasket hole, or to stand on edge. Use of a single-camel-hair probe is often essential for intact loading of such specimens.

All runs in the present SL experiments are calibrated using multiple ruby chips as described in Paper I. The quoted pressures refer to interpolated R-line values[42] at the particular specimen sites being probed. As in the bulk measurements, the interpolation precision for a well-annealed alcohol medium is estimated to be ±0.4 GPa, by comparing to the measured pressure shift of each specimen's GaAs LO(Γ) Raman peak. Now, however, this comparison is based on the least-square fit in Fig.

TABLE I. Summary of sample characteristics and observed pressures for forward and reverse transitions. P_1^t and P_2^t denote the first (AlAs) and second (GaAs) thresholds on increasing pressure. R^t denotes the pressure at which transparency returns on decompression. Values in brackets correspond to reversal of only the AlAs component. The analogous forward thresholds in bulk AlAs (BL1) and GaAs (BL2) are 12.4±0.4 GPa and 17.3±0.4 GPa, respectively. (See Paper I.)

Samples	SL1	SL2	SL3	SL4	SL5	SL6
GaAs/AlAs	165 Å/290 Å	225 Å/75 Å	200 Å/50 Å	50 Å/25 Å	50 Å/20 Å	25 Å/60 Å
Periods	60	73	80	250	100	200
Growth	OMCVD	MBE	MBE	MBE	MBE	OMCVD
P_1^t (GPa)	13.8±0.4	14.6±0.4	16.0±0.4	17.2±0.4	17.1±0.4	16.9±0.4
P_2^t (GPa)	16.8±0.8	17.4±0.8	17.3±0.8	17.2±0.4	17.1±0.4	16.9±0.4
R^t (GPa)	8.2±1.5		8.8±1.5	6.0±1.5	6.4±1.5	11.5±1.5
	[8.5±1.5]	[9.2±1.5]				

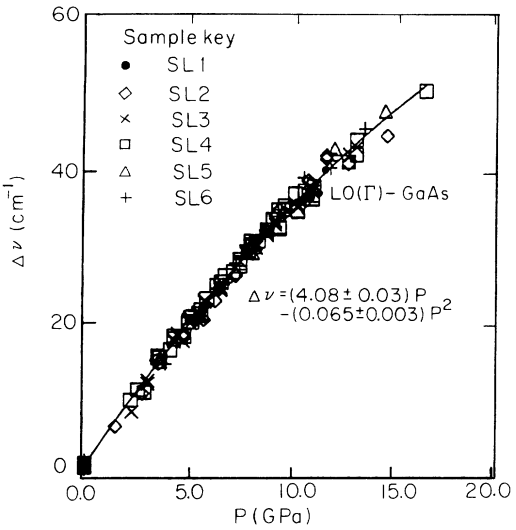

FIG. 5. Pressure-induced shift of the GaAs LO(Γ) frequency measured for SL1–SL6. Equation gives least-square fit (solid curve) used to corroborate ruby-calibrated pressures.

5 (solid curve), which represents, within statistical error, *all* of our pretransition data from over 200 measurements on SL1–SL6.[41] In the hydrostatic region, this "universal" SL fit agrees well (but not identically) with the BL2 calibration used in Paper I. However, for the SL's it corresponds more closely to the interpolated ruby results above 9.5 GPa, where pressure gradients increase the data scatter (see Fig. 5). The best linear-fit Grüneisen parameters corresponding to these LO(Γ) data, and to the measured pressure shifts of other prominent phonons in the SL samples are listed in Table II. Reasonable agreement is found with previous reports.[41,43,44]

As remarked, it is possible to have either separate or simultaneous AlAs and GaAs transitions in the SL samples. For those SL's undergoing separate changes, the lower pressure threshold at P_1^t is detected by both the onset of visual opacity and the simultaneous disappearance of the ZB AlAs, but not the GaAs, Raman peaks. The higher P_2^t threshold can then be detected only by the vanishing of the GaAs Raman peaks, with no visual change apparent in the already opaque specimens. Two independent DAC runs were carried out for all the SL's, during which each was held, at least once, in a partially transformed phase, i.e., mixed transparent-opaque state. [See for example, Fig. 1(c).] The procedures and precautions for determining the thresholds are the same as described in Paper I, and the variation in the measured P_1^t is again comparable to the ruby precision, ±0.4 GPa. Our results for P_2^t are less certain, because inability to view the onset of opacity by eye increases the tendency to overshoot this transition. Nevertheless, the use of small pressure steps followed by annealing effectively limits the uncertainty to ±0.8 GPa for P_2^t. The estimated accuracy for the SL reverse thresholds R^t is ±1.5 GPa (as for BL1 and BL2 in Paper I) due to the larger steps employed during decompression.

IV. EXPERIMENTAL RESULTS

In this section we present Raman-scattering spectra for the AlAs/GaAs SL's listed in Table I at various pressured cycled up and down through their phase transitions. These Raman data, in combination with our visual observations, reveal a great deal. In particular, they allow us to establish for the AlAs/GaAs system the experimental situation concerning three crucial questions: Under what circumstances do separate transitions occur in the AlAs and GaAs layers; to what extent do AlAs overpressing *and* GaAs underpressing occur; what is the post-transition condition of the heterointerfaces? It will be helpful to keep these central questions in mind while considering the body of data presented below.

The SL samples fall quite naturally into two categories—thick layer, and thin layer. While it is fairly clear that any film of thickness greater than 0.3 μm (~1000 monolayers) should be considered bulklike, the distinction between thick- and thin-layer SL's is more vague, and is determined here by whether the SL constituents are observed to undergo separate or simultaneous α-β transitions, respectively.

A. Separate versus simultaneous GaAs and AlAs transitions in SL's

As discussed in the Introduction, evidence for separate AlAs and GaAs α-β phase changes within a SL came from visual studies revealing the onset of opacity in SL1 via discrete sudden steps at constant pressure.[7] Subsequent optical-microscopy experiments showed sudden (i.e., <0.1 sec) stepwise transitions in both SL1 and SL2, but found that less uniform pressure environments could cause the steps to ensue in well-defined macroscopic

TABLE II. Linear Grüneisen constants γ for the AlAs-like and GaAs-like phonons observed in SL1–SL6. Estimated uncertainties are indicated for each mode type.

	GaAs-like modes			AlAs-like modes	
Sample	$\gamma_{LO(\Gamma)}$	$\gamma_{TO(\Gamma)}$	$\gamma_{2TA(X)}$	$\gamma_{LO(\Gamma)}$	$\gamma_{TO(\Gamma)}$
SL1	1.09±5%	1.22±5%		1.06±10%	1.68±10%
SL2	1.05	1.32		0.97	
SL3	1.09	1.27	−1.04±8%	0.92	1.39
SL4	1.08	1.21	−1.07	1.05	1.47
SL5	1.05				
SL6	1.05			0.96	

domains within the SL plane, instead of homogeneously across the specimen surface as in the previous work. This is illustrated for SL2 in Fig. 1(c), where the domains exhibit some tendency to grow along ZB-phase [110] directions. However, the momentary nature of the changes prevents us from studying such growth patterns in detail. The occurrence of *stepwise* darkening below P_g^t strongly indicates separate AlAs and GaAs transitions in SL1 and SL2, placing these samples in the thick-layer category. For SL3 visual microscopy does not reveal sudden stepwise transitions. Instead, the transformation kinetics at P_1^t are more sluggish, with the transparent-opaque phase boundary expanding at an apparently continuous rate of a few μm/min. Although this resembles the transition kinetics described below for the thin-layer SL's, and also that found for bulk GaAs (see Paper I), we shall see that the Raman results place SL3 in the thick-layer group as well.

The sequential evolution of the one-phonon Raman spectra in the thick layer SL's, for pressure increasing through their initial P_1^t and P_2^t transitions, is shown in Figs. 6–8. The displayed 1 bar traces are taken on substrate-backed samples outside the DAC. They are quite typical of GaAs/AlAs SL's with similar layer dimensions, exhibiting the allowed LO(Γ) peaks of GaAs and AlAs near 292 and 403 cm^{-1}, respectively, and subsidiary structure at lower frequency due to confined overtones, interface modes, and forbidden TO(Γ) scattering. The latter have been studied extensively at 1 atm.[39,45]

The upper two or three panels of Figs. 6–8 give the key results for α-β transitions in the thick-layer SL's. These data show that at the various P_1^t thresholds, where opacity first sets in, the ZB AlAs spectrum is essentially absent from darkened portions of the samples but present in transparent regions. [Compare the traces in panels 6(c) and 6(d), 7(c), 8(c) and 8(d) in relation to the inset sketches showing sample morphology and laser position.] In contrast, the ZB GaAs peaks do not disappear until P exceeds 17.3±0.8 GPa. Thus, the discrete transitions observed visually in SL1 and SL2 can correspond to the α-β transition of only the AlAs layers, and not the GaAs layers. The latter transform separately at pressures P_2^t close to the bulk GaAs threshold P_g^t. Further, it is clear from

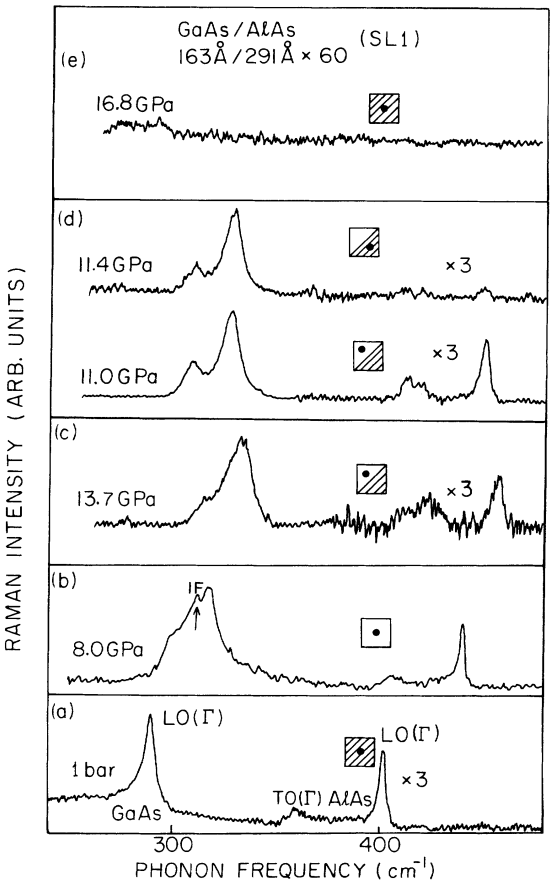

FIG. 6. Pressure-Raman chronicle for SL1 showing changes in the GaAs and AlAs one-phonon ZB spectra due to the separate α-β transitions in each constituent. Square insets depict sample's opaque or transparent state and laser position. (a) 1 bar. Note labeled assignments. (b) 8.0 GPa. Pretransition resonant Raman result showing GaAs-like interface peak (IF). (c) and (d) 13.7 and 11.0–11.4 GPa. AlAs began to transform in (c), and pressure was then dropped to ensure capture (due to hysteresis) of mixed state in (d). Note, GaAs *and* AlAs peaks persist in transparent areas, but opaque portions show only GaAs peaks. (e) Pressure was increased through $P_1^t = 13.8 \pm 0.4$ GPa (when complete opacity set in) to 16.8 GPa. GaAs peaks now vanish.

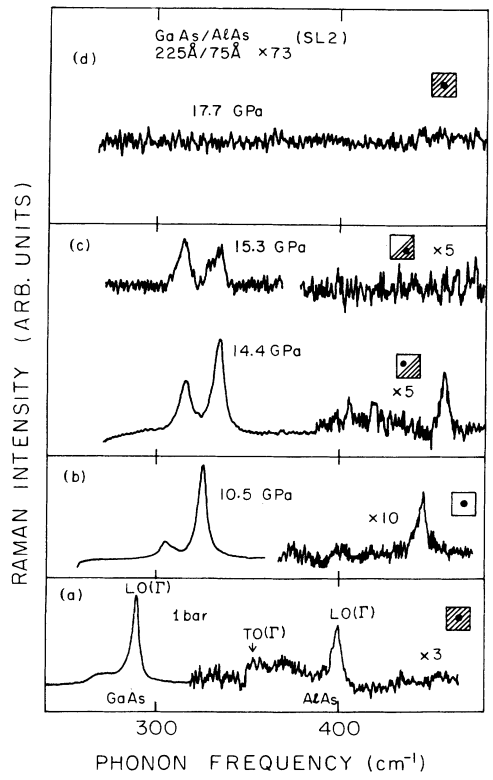

FIG. 7. Sequential Raman study under increasing pressure of separate α-β transitions in SL2. The AlAs peaks vanish with the onset of opacity in (c), but the GaAs peaks persist until P_2^t is exceeded in (d). Pressures are ruby values interpolated to the laser spots.

the Fig. 8 Raman results that separate AlAs and GaAs transitions also occur in SL3, even though its transition kinetics are continuous and more sluggish.

The above behavior is to be contrasted with that found for the phase transitions in the thin-layer samples, SL4–SL6. The visible morphology and kinetics of these transitions are similar to what is observed for SL3 and for bulk semiconductors (see Paper I)—continuous expansion of one or more opaque nucleation regions at the rate of a few μm/min. In earlier work on SL5, this bulklike kinetics and the fact that $P_1^t \approx P_g^t$ (unlike SL3, see Table I) was interpreted to signify simultaneous AlAs and GaAs transitions.[7,22]

Figures 9–11 present pressure-Raman data for SL4–SL6, respectively. Again the 1 bar spectra are quite typical, showing instances of fairly strong interface and/or confined-mode structure between the allowed LO(Γ) and forbidden TO(Γ) peaks.[39,45] For SL5, smaller total thickness compared to SL4 and SL6 reduces the overall intensity, especially for AlAs scattering in the DAC (see Fig. 10 for $P > 0$). Panels 9(d), 10(c) and 10(d), and 11(c) focus on transition-induced effects. These data show explicitly that the lowest-pressure α-β transition in SL4 and SL6 is accompanied by simultaneous disappearance of *both* the AlAs and GaAs ZB spectra at the onset of opacity. The results for SL5 show the transition-induced vanishing of only the GaAs ZB peaks because AlAs scattering could not be observed at elevated pressure. However, we may be sure that the AlAs and GaAs transitions again are concurrent, since transparency is maintained until the GaAs peaks vanish, and there is no instance in any SL of the AlAs threshold exceeding P_g^t. (Nor is there any physical reason for this. See Sec. II.) SL5 is also notable for exhibiting a broad amorphous-GaAs-like spectrum just above threshold.[46] This appears in the Fig. 10(d) and 10(e) traces measured in two separate DAC loadings. SL5 is the only sample for which we could reproducibly observe any Raman spectra in the opaque high-pressure phase.

The effect of retaining the substrate has been explored for SL4. This was motivated by a report of a 12-GPa AlAs transition in a substrated SL having layer thickness in the "thin layer" category.[43] Such a threshold disagrees with the present thin-layer SL results by some 5 GPa, and, since it is $\sim P_a^t$, contradicts the general stability trends observed here. Figure 12 compares corresponding Raman data for substrated and free-standing specimens of SL4. The two specimens are seen to behave similarly, each exhibiting simultaneous transitions of their AlAs and GaAs components above 16.5 GPa.

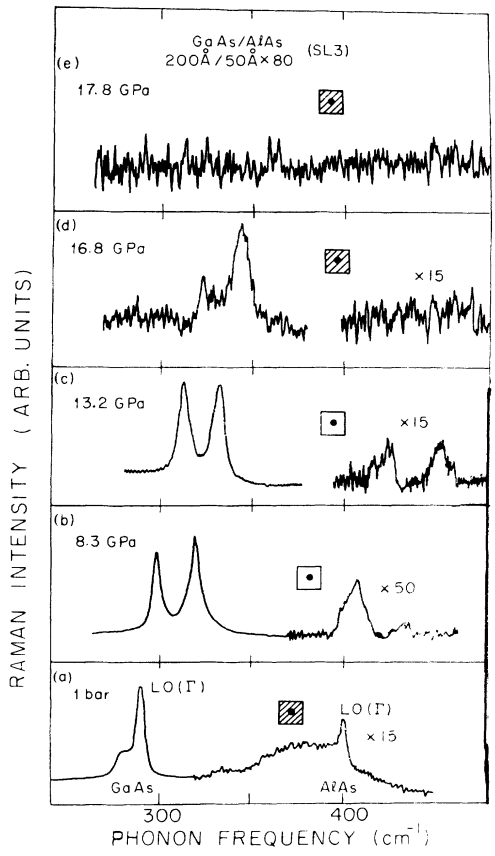

FIG. 8. Raman chronicle of α-β phase changes in SL3 (as in Figs. 6 and 7 above). Again the AlAs component disappears above the P_1^t threshold (16.0 GPa, see Table I) in (d), but the GaAs peaks remain until pressure exceeds $P_2^t = 17.3$ GPa in (e).

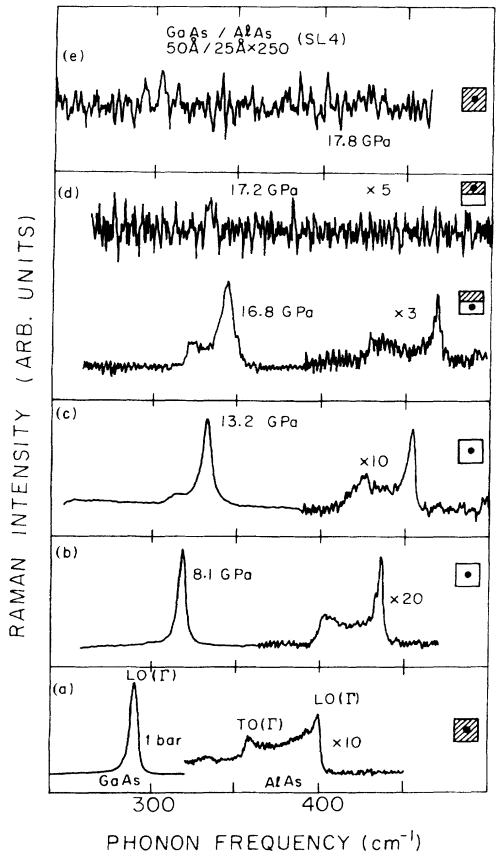

FIG. 9. Sequential pressure-Raman data showing *simultaneous* AlAs and GaAs α-β phase changes in SL4. (a)–(d) Zinc-blende spectra of AlAs and GaAs persist until 17.2 GPa, when both disappear with the onset of opacity, as in (d) and (e).

B. Overpressing of AlAs and underpressing of GaAs

The average observed threshold pressures P_1^t and P_2^t for α-β transitions of the AlAs and the GaAs layers in SL1–SL6 are listed in Table I. We emphasize: For the thick-layer samples, SL1–SL3, P_1^t exceeds the bulk AlAs threshold $P_a^t = 12.4$ GPa by 1.4, 2.2, and 3.6 GPa, respectively; furthermore, for the thin-layer samples, SL4–SL6, the various P_1^t are each within 0.5 GPa of the bulk GaAs threshold $P_g^t = 17.3$ GPa. In contrast, P_2^t is essentially sample independent, so that within experimental error the GaAs layers of all the SL's transform at the bulk GaAs threshold. These results confirm the previously observed trends for overpressing of ZB AlAs in GaAs/AlAs SL's (Refs. 7 and 22)—that such overpressing increases with decreasing AlAs layer thickness until, for sufficiently thin layers, a single transition of both constituents occurs at a threshold near the stability limit of bulk ZB GaAs. Furthermore, the Raman data establish that there is essentially *no complementary underpressing* of GaAs below its bulk stability limit.

Our experimental findings are summarized in Fig. 13, where the extent of AlAs overpressing and GaAs underpressing can be assessed by the distances of the crosses above P_a^t, and of the squares below P_g^t, respectively. This figure is a key result, whose understanding we shall seek in terms of the macroscopic theory of heterointerface energetics developed in Sec. II. Figure 13 shows experimentally that the ultimate stability of GaAs/AlAs SL's against hydrostatic compression (at 300 K) is *controlled by GaAs,* i.e., by the SL constituent with the higher α-β transition pressure. This conclusion is intriguing for applications of mismatched or metastable heterostructures, as we discuss below in Sec. VI.

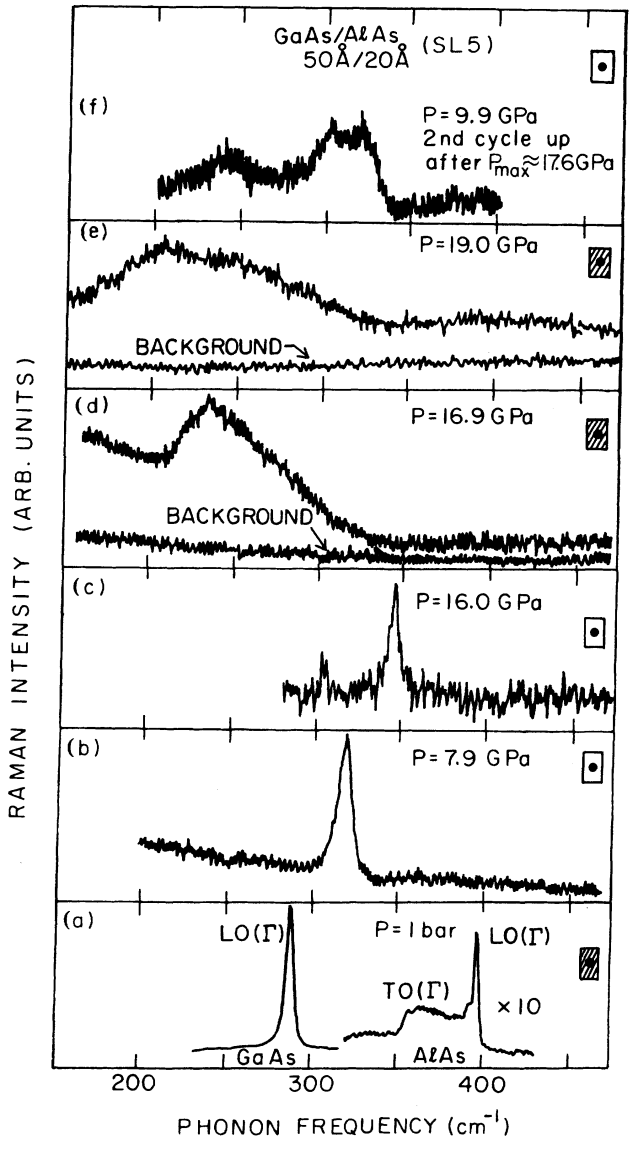

FIG. 10. Raman study of forward and reverse high-P phase changes in two DAC loadings of SL5. Only GaAs scattering could be observed in the DAC. Zinc-blende LO(Γ) peak persists in (a)–(c), until in (d) at 16.9 GPa, it is replaced by a broad amorphous GaAs-like band (see Paper I, Fig. 6). (e) Second SL5 specimen shows similar (but broader) transformed-state spectrum. (f) Transparent-phase data for first specimen after the pressure cycle 17.6→0.3→9.9 GPa. Broadening between LO(Γ) and TO(Γ), and residual β-phase band, reveal interface and bulk disorder and incomplete reversal.

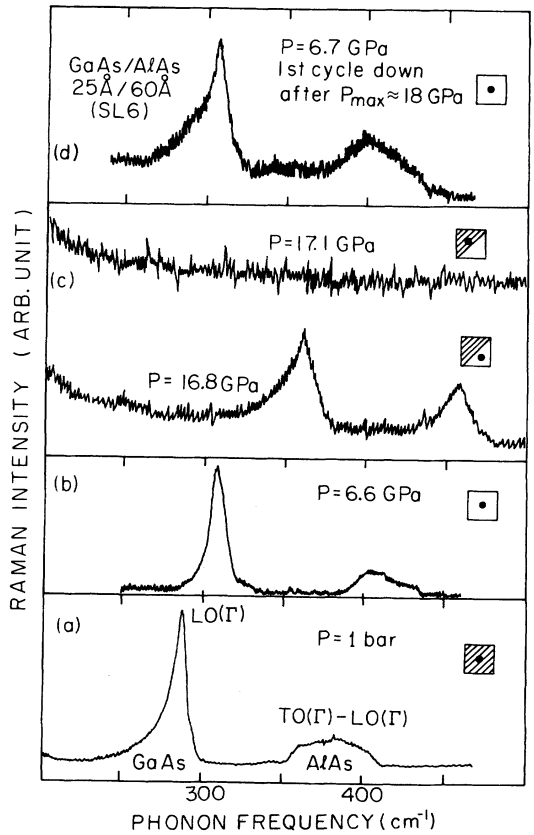

FIG. 11. Raman chronicle of forward and reverse transitions in SL6. GaAs and AlAs ZB spectra are observed in (a) and (b) until in (c) they both disappear (17.1 GPa) or both persist (16.8 GPa) in the opaque or transparent regions, respectively. (d) Transparent-phase spectrum after cycling (18.0→6.7 GPa) through reversal to ZB phase. Compare with (b).

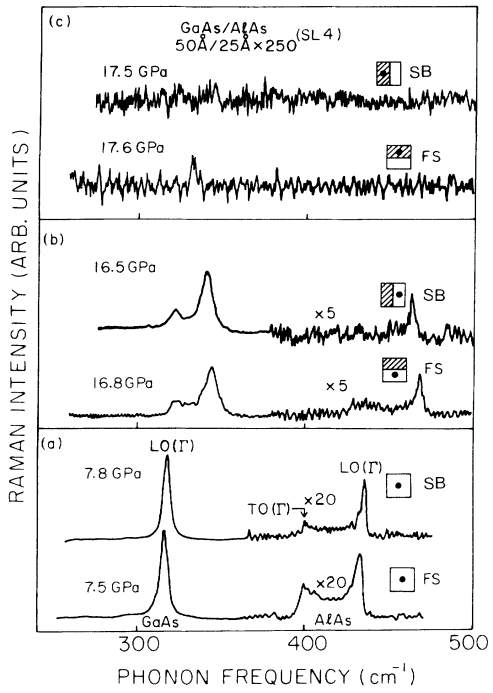

FIG. 12. Pressure-Raman comparison of α-β transitions in free-standing (FS) and substrated (SB) specimens of SL4. In each, the AlAs and GaAs peaks disappear at essentially the same threshold.

C. Transition reversal

On decompression after undergoing their α-β transitions, all the SL's studied here regain transparency as long as the maximum up-cycle pressure P_{max} does not exceed ~20 GPa. (When $P_{max} > 20$ GPa, a metastable phase similar to that found in bulk GaAs appears in the SL's.[47] This is the same circumstance discussed in Paper I.) The observed transparency-return thresholds are given as R^t in Table I. There is always 6–8 GPa threshold hysteresis with respect to the original increasing-pressure transitions. Threshold hysteresis in the SL's, as in bulk samples, arises from the nucleation mechanism of the α-β transformation.[28,48] Often samples that regain transparency exhibit morphological imperfections, e.g., translucent regions, blemishes, or an increased brownish color compared to their pretransformed condition at the same pressure. An example is shown in Fig. 1(e) for SL2. Such markings probably are associated with macroscopic grain boundaries and/or incomplete reversal.

To investigate whether the R^t transparency thresholds observed in SL1–SL6 actually correspond to reversal, i.e., the return of the ZB phases in both the AlAs and GaAs layers, we compare Raman results recorded before and after cycling the SL's through their P_1^t, P_2^t, and R^t transitions. The comparisons are given for the thick-layer SL's in Figs. 14–16, and for the thin-layer SL's in Fig. 17, and Figs. 10 and 11 (introduced earlier). We find that in every case where transparency returns, so also do the ZB Raman peaks of the transformed constituent(s). Often the cycled spectra are weaker, somewhat broader, and exhibit revealing signs of interface degradation (to be discussed below), but the ZB GaAs and AlAs signatures are unmistakable.

Figures 14(b) for SL1 and 15(b) for SL2 show instances where GaAs did not transform out of its ZB phase, viz., $P_{max} < P_2^t$, so that the observed reversals are confined to

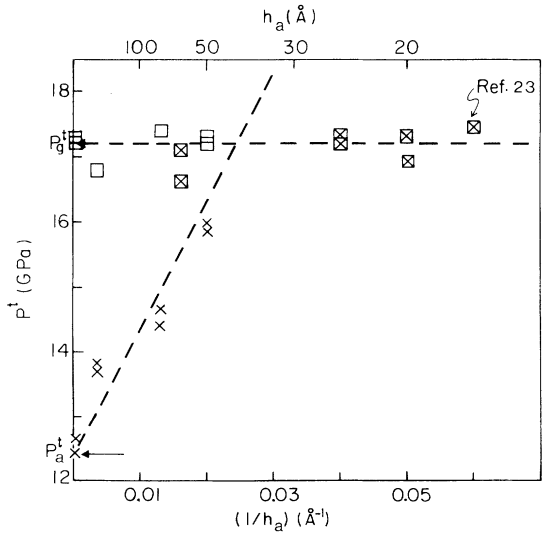

FIG. 13. Measured α-β transition pressures P_1^t for AlAs (crosses) and P_2^t for GaAs (squares) in SL1–SL6. Bulk P_a^t (AlAs) and P_g^t (GaAs) thresholds from BL1 and BL2 in Paper I are marked by arrows and the horizontal dashed line. Sloped dashed line is linear fit to P_1^t in the "thick-layer" regime. Scales are the same as in Fig. 2 for comparison. Datum at 0.06 Å^{-1} after Ref. 23.

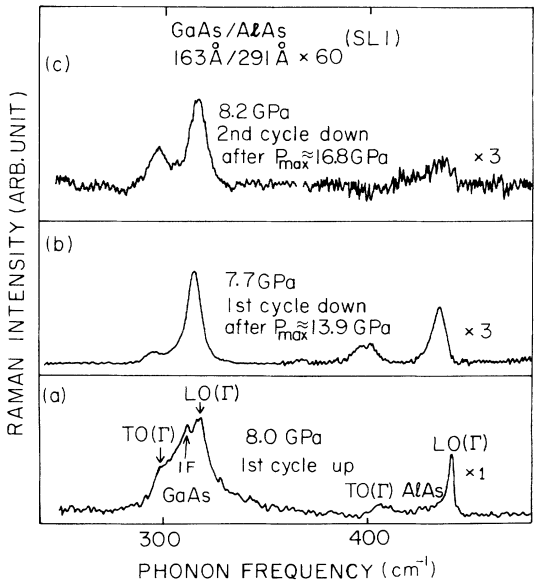

FIG. 14. Pressure-cycling comparison of pretransition and postreversal spectra in SL1. (a) 8.0 GPa. Initial ZB resonant Raman ($\lambda_l = 568$ nm) spectrum showing interface peak (IF) between GaAs LO(Γ) and TO(Γ). (b) 7.7 GPa, after only AlAs transformed. (c) 8.2 GPa, after both AlAs *and* GaAs transformed. Clear ZB signatures for GaAs and AlAs appear in (b) and (c), but the GaAs-like interface peak does not survive.

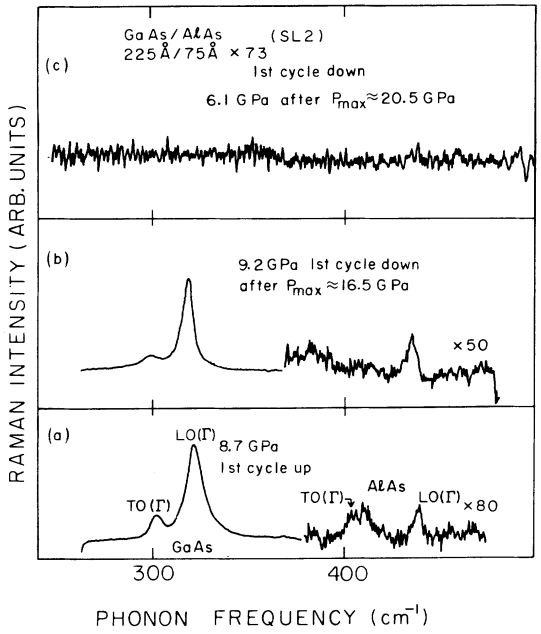

FIG. 15. Pressure-cycling comparison for SL2, similar to Fig. 14. (a) 8.7 GPa, pretransition. (b) 9.2 GPa, after only AlAs transformed. Return of ZB AlAs LO(Γ) peak is seen. (c) 6.1 GPa, cycled from $P_{max}\sim 20.5$ GPa. Sample is in an opaque metastable state showing no measurable Raman spectrum.

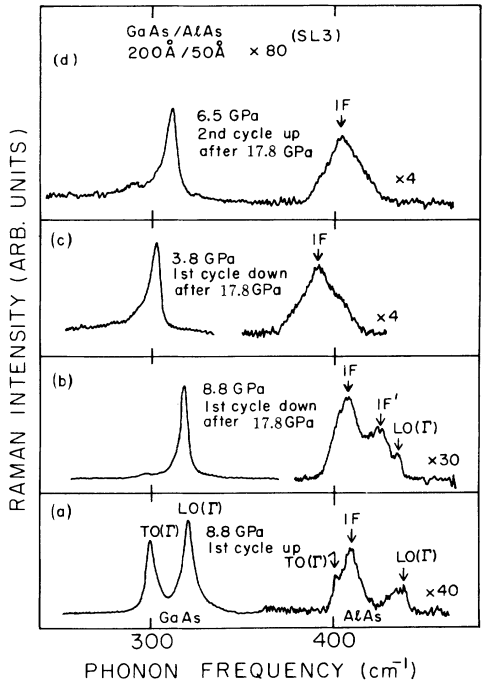

FIG. 16. Pressure-cycling study for SL3. (a) 8.8 GPa, pretransition. Note AlAs-like interface mode (IF). (b) 8.8 GPa, first cycle down after AlAs and GaAs transformed. Zinc-blende features reappear, including two strong IF peaks. (c) and (d) evolution of spectra as pressure is lowered to 3.8 GPa, then raised to 6.5 GPa. Broadening of IF modes indicates increased interface disorder.

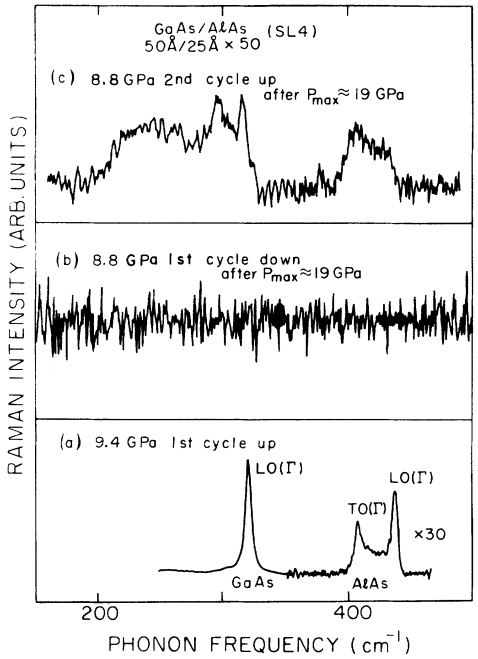

FIG. 17. Pressure-cycling comparison for SL4. (a) 9.4 GPa, pretransition. (b) 8.8 GPa, after AlAs and GaAs transformed. Sluggish reversal has not yet occurred. (c) 8.8 GPa, second cycle up from $P_{min}=0.8$ GPa. Returning ZB LO(Γ) and TO(Γ) peaks are obscured by broadbands implying bulk and interface disorder. Note similarity to Fig. 10(f).

the AlAs layers. In contrast, Fig. 14(c) records the return of both ZB AlAs and ZB GaAs in SL1, whereas in Fig. 15(c) for SL2 neither constituent undergoes reversal because P_{max} has exceeded 20 GPa. The other depicted cases pertain to SL3–SL6, and correspond to reverse transitions of both the AlAs and GaAs constituents. Note that the postreversal spectra of SL4 and SL5 [Figs. 17(c) and 10(f)] acquire a mixed character, consisting of ZB GaAs and AlAs peaks, and a broadband in the GaAs frequency region. For SL5 this band appears to survive from the β-phase spectra presented in Figs. 10(d) and 10(e). These variations not withstanding, we find for the SL's, as for the bulk films (Paper I), that the return of transparency at R' coincides with reversal to the ZB phase within substantial fractions of the AlAs and/or GaAs constituents.[49]

D. Degradation of the heterointerfaces

The condition of the SL heterointerfaces after a cycle of transition and reversal is important because it bears on our decision between the DI and the FE limits. Considering the large volume and coordination changes that occur in bulk α-β transitions (Paper I), one expects some interface degradation in SL's. The relevant questions are how much degradation, and how does it relate to the occurrence of separate or simultaneous AlAs and GaAs phase changes.

The Raman data are quite telling for SL1, because its pretransition spectrum under resonant excitation at 8.0

GPa exhibits strong scattering from interface and confined modes between the GaAs TO(Γ) and LO(Γ) frequencies [see Fig. 14(a)]. However, this scattering no longer appears in SL1 after reversal from stepwise transitions of only its AlAs layers [Fig. 14(b) at 7.7 GPa], nor after a second pressure cycle in which both constituents separately transform [Fig. 14(c) at 8.2 GPa]. Hence, in this "thick-layer" SL there is clear Raman evidence for transition-induced degradation of the heterointerfaces.

A similar comparison for SL2 [Figs. 15(a) and 15(b)] is not very revealing, concerning interface degradation because this sample does not exhibit strong interface scattering before transforming. Figure 15(c) illustrates a case where $P_{\max} \geq 20$ GPa, so that SL2 returns to low pressure in an opaque metastable state showing no measurable Raman spectrum inside the DAC.

For SL3, a pronounced AlAs-like interface peak is observed before the transformation under direct gap resonance. This is the 415 cm^{-1} peak labeled IF in Fig. 16(a). After increasing pressure through the separate transitions of the AlAs and GaAs layers, and then cycling back to 8.8 GPa from $P_{\max} = 17.8$ GPa, the ZB spectrum of SL3 still contains the original IF peak [Fig. 16(b)]. However, broadening has increased the overlap with TO(Γ), and a second interface peak IF′ has developed at 430 cm^{-1}. The broadening increases further on lowering pressure to 3.8 GPa and recycling to 6.5 GPa [Figs. 16(c) and 16(d)], until the AlAs spectrum exhibits a single triangular peak centered between TO(Γ) and LO(Γ). Such broadening[39,45] strongly suggests transition-induced interface disorder that has continued to grow during the ~20 h of the cycling process. Concurrently, the GaAs LO(Γ) peak in SL3 shows little change in width; however, the GaAs forbidden TO(Γ) peak virtually disappears, probably due to attenuation of forward scattering (see Paper I) from increased specimen cloudiness.

The thin-layer SL's also exhibit strong transition-induced disorder effects. These are apparent in the post-reversal Raman spectra of SL4 and SL5 [Figs. 17(c) and 10(f)], and particularly in the two β-phase traces measured for SL5 at 16.9 and 19.0 GPa [Figs. 10(d) and 10(e)]. In each, we find broad structureless bands below the GaAs TO(Γ) frequency that resemble the 150–300 cm^{-1} spectrum of sputtered amorphous GaAs reproduced after Zallen *et al.*[46] in Fig. 6(d) of Paper I.[50] These spectra suggest that the disorder is not confined to the interfaces, since broadening would then occur mainly between the TO(Γ) and LO(Γ) frequencies of GaAs and/or AlAs, as in the thick-layer SL's. Indeed, for SL4 and SL5, it is easy to imagine "interface" disorder extending over substantial fractions of the layers which are only 20–50 Å thick. In contrast, a similar broadband does not appear to develop in SL6 [Fig. 11(d)]. Although this may stem from the layer-thickness ratio being inverse to that in SL4 and SL5 (i.e., more AlAs, see Table I), it is somewhat puzzling at present. Nevertheless, the weight of our evidence shows that transition-induced disorder effects become increasingly important in SL's with thinner layers.

It was noted earlier that when $P_{\max} \geq 20$ GPa, both bulk and SL samples return to 1 bar in an opaque metastable state. Detailed studies of this state in BL1, BL2, SL2, and SL4 show similar non-ZB Raman spectra in the GaAs frequency range and no AlAs scattering. (See also Paper I, Sec. III D.) The point to emphasize here is that such bulklike behavior in GaAs/AlAs SL's suggests that the initial α-β transformation can produce sufficient interface degradation to relax epitaxial constraints on subsequent decreasing-pressure transitions.

E. Summary of principal experimental results for SL phase transitions

The present Raman measurements combined with visual observations have established the following key points, which we review before embarking on further discussion in terms of the theory in Sec. II.

Pressure-induced transitions in AlAs/GaAs SL's take place in two qualitatively different ways. The transformations occur either separately in each layer type, or simultaneously in both layer types, and it is possible to group the SL's, respectively, into thick-layer and thin-layer categories according to this behavior. Transitions in the former group often proceed with rapid (<0.1 sec) kinetics within individual layers, while in the latter group one finds sluggish (~ min) expansion of multiple nucleation sites. The AlAs transition pressure in SL's depends strongly on the thickness of the AlAs layers, increasing from the bulk AlAs threshold $P_a^t = 12.4$ GPa to the bulk GaAs threshold $P_g^t = 17.3$ GPa with decreasing thickness according to Fig. 13. This overpressing of ZB AlAs is not matched by a complementary underpressing in GaAs, which transforms very close to P_g^t regardless of the thicknesses of the GaAs or the AlAs layers in the samples studied. The α-β transitions in SL and bulk samples alike can be made to reverse on decompression with 6–8 GPa hysteresis provided $P_{\max} < 20$ GPa. After reversal, the ZB Raman spectra of the SL's show increasing signs of interface degradation and disorder as one progresses from the thickest-layer to the thinnest-layer SL's. A metastable microcrystalline phase of GaAs, different from its ZB and amorphous varieties, occurs both in AlAs/GaAs SL's and in bulk GaAs, whenever specimens are returned to 1 atm after pressurization above 20 GPa.

V. DISCUSSION

The fact that the pressure-induced structural transitions of two-constituent SL's may occur either separately or simultaneously in each constituent, according to whether the SL layers are thick or thin, is not surprising. This qualitative distinction must apply in the two extreme situations of infinite layer thicknesses, for which each layer's bulk properties should not be altered by neighboring layers, and of atomic monolayers, for which alloylike behavior is expected. A similar distinction, based on the concept of critical thickness to form misfit dislocations, has achieved wide acceptance in theories of equilibrated pseudomorphic growth.[13,14,25] What is surprising about the crossover from separate to simultaneous transitions is the observed dependence on the layer thicknesses of both constituents. Namely, it is

difficult to understand why neither the GaAs nor the AlAs thresholds are influenced appreciably by the GaAs layer width, while the AlAs threshold depends strongly on the AlAs layer width until crossover occurs at $h_a \sim 40-50$ Å. This leads to the absence of GaAs underpressing in the presence of AlAs overpressing, so that *the SL stability against the α-β transition tends to be GaAs dominated* even in cases where the mole-fraction of GaAs to AlAs is substantially less than unity.

Comparing the measured behavior of P_1^t and P_2^t versus $1/h_a$ in Fig. 13 with the predictions of the FE, the DI, and the EA limits in Fig. 2, it is clear that the DI limit corresponds most closely to our observations. We, therefore, envision a model in which the P_1^t transition induces a dense tangled net of interface dislocations sufficient to relieve all homogeneous strain and to produce considerable interface disorder. In this view the lowest pressure transition is a catastrophic event, in which the large lattice-constant and coordination-number changes in the AlAs layers relax any pseudomorphic constraints for the subsequent P_2^t transition in the GaAs layers. Essentially the same level of interface disorder persists after the P_2^t transition because the low (300 K) temperature inhibits annealing and diffusion processes that could otherwise reduce the density of interface dislocations in the β/β phase. Our Raman observations of increasing interface disorder with decreasing layer thickness in SL's undergoing reversal offer additional support for this picture. The situation is quite different from epitaxial growth of mismatched SL's, where one often assumes that the temperature is high enough and the process "gentle" enough to allow extensive migration of dislocations.[14]

To further assess the validity of the DI limit, let us examine the measured AlAs overpressing more quantitatively. According to Eq. (6), the linear slope describing P_1^t as a function of $1/h_a$ within the thick-layer regime in Fig. 13 gives an empirical value for the change in the interface energy density $(\sigma^{\beta\alpha}-\sigma^{\alpha\alpha})$ at the $\alpha/\alpha \rightarrow \beta/\alpha$ transition. Then, assuming $\sigma^{\alpha\alpha}$ can be neglected for the initially lattice-matched AlAs/GaAs system [this is confirmed by microscopic calculations showing $\sigma^{\alpha\alpha} \sim 10^{-3}$ eV/Å^2 (Ref. 26)], and taking the typical value -18% (Refs. 3 and 33) for the volume decrease in bulk AlAs, we obtain $\sigma^{\beta\alpha}=0.12\pm0.02$ eV/Å^2.

This is a key experimental result with several interesting implications. It is compared with the predictions of Martin's[7,8] total-energy calculation for a sixfold-fourfold SL in Fig. 18. The left-hand ordinate in this figure, labeled $\Delta(H/V_0)$, gives the enthalpy per unit volume (or per atom on the right) of either AlAs or GaAs in a rocksalt β phase that is subject to possible pseudomorphic constraints. At each pressure this quantity is calculated relative to the material's enthalpy density (or atomic enthalpy) in the normal ZB α phase for which the $P=0$ volume is V_0. Hence, α-β transitions are predicted when $\Delta(H/V_0)=0$. As defined, $\Delta(H/V_0)$ is

$$\Delta\left[\frac{H}{V_0}\right]=\frac{1}{V_0}[(U_a^{\beta}+U^{\beta\alpha}+PV_a^{\beta})-(U_a^{\alpha}+PV_a^{\alpha})] , \quad (14)$$

where the symbols have the same meanings as in Sec. II.

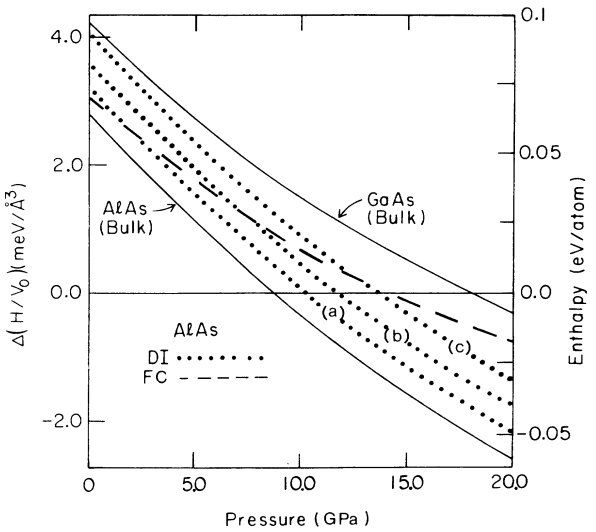

FIG. 18. Calculated enthalpies of rocksalt (B1) AlAs and GaAs for different relaxed and constrained geometries relative, at each pressure, to the corresponding bulk ZB phases. Solid and dashed curves, due to a theory by Martin (see Refs. 7 and 8), describe total energy results for, respectively, bulk material, and B1 AlAs fully constrained (FC) to match ZB GaAs at a (111) sixfold-fourfold interface. Dotted curves give the expected dependence in the DI limit for AlAs layer thicknesses of (a) 290 Å, (b) 145 Å, and (c) 95 Å. (See Secs. II and V.)

Using Eq. (3), and again neglecting second-order terms, we obtain for AlAs

$$\Delta\left[\frac{H}{V_0}\right]=\frac{\sigma^{\beta\alpha}}{h_a}+(P-P_a^t)(\Delta V/V)^{\beta\alpha} , \quad (15)$$

and similarly for GaAs by a change in subscripts. The solid curves in Fig. 18 are for $\sigma^{\beta\alpha}=0$, and, hence, pertain to bulk material. The predicted bulk thresholds are 17 GPa for GaAs and 9 GPa for AlAs, indicating the reasonable accuracy of this calculation.[6,8] The dashed curve corresponds to the calculated result for sixfold rocksalt AlAs fully constrained (FC) to match fourfold ZB GaAs at a (111) interface with no dislocations; the predicted transition in this case is at 14.8 GPa. The series of dotted curves represents the DI limit. In this case, the empirical value of $\sigma^{\beta\alpha}$ obtained above should apply, and, according to Eq. (15), at $P=P_a^t$ each dotted curve should pass through a point located a distance $\Delta(H/V_0)=(0.12/h_a)$ eV/Å^3 above the abscissa. Since the dislocation density in this limit is large enough to relax pseudomorphic constraints in the β/α phase, an approximate representation at *all* pressures may be obtained by a uniform vertical displacement of the bulk AlAs curve through this distance. We note that for realistic values of h_a the dotted curves fall between the bulk GaAs and bulk AlAs boundaries, as required on physical grounds.

Figure 18 shows that, with decreasing AlAs layer thickness, the DI limit will eventually become less favorable than Martin's strained pseudomorphic sixfold-fourfold configuration. This will occur for a value of h_a

such that the dashed and dotted curves cross each other at the abscissa—$h_a \approx 90$ Å in Fig. 18. This is a factor of two larger than the observed 40–50 Å onset thickness for direct transformation to the β/β phase *via simultaneous* GaAs and AlAs transitions (i.e., the crossover in Fig. 13). Hence, a stable strained-layer β/α structure might be possible in AlAs/GaAs SL's for 50 Å $< h_a <$ 90Å. However, we find no evidence for this, since the Raman results in Figs. 7(c) and 8(d) fail to show a ZB GaAs spectrum under strong biaxial strain subsequent to the transition in the AlAs layers. Nevertheless, for other materials systems a pseudomorphic strained-layer β/α phase, where the nearest-neighbor coordination changes discontinuously from fourfold to sixfold, remains a physical possibility that should not be categorically discounted.

In order to attribute the mechanism for AlAs overpressing specifically to transition-induced misfit dislocations at the β-AlAs/α-GaAs interfaces, we inquire whether the measured interface energy density reflects a realistic concentration $(1/\lambda_d)$ of such dislocations. The value $\sigma^{\beta\alpha}=0.12$ eV/Å^2 corresponds to 0.085 eV/Å for each lattice plane cutting orthogonally through a ZB (001) interface (viz., $\sigma^{\beta\alpha}$ is distributed over two directions each containing four normal planes per a_0, with $a_0=5.653$ Å for GaAs at 1 bar.) In order to obtain λ_d, the empirical result 0.085 eV/Å may be compared with the energy per unit length of each misfit dislocation, given by the expression within curly brackets in Eq. (8). Instead of the standard isotropic-medium expression for $\mu/(1-\nu)$, we employ the more accurate formula given by Read and Shockley for a (001) interface,[51] and we also adopt the core contribution $C=0.23$ deduced from experiment by these authors. Then, replacing $\ln(\sqrt{h_a h_g})$ by its average for the three thick-layer SL's (the error incurred by averaging is less than 10%, see Table I), using the AlAs elastic constants,[30] and taking $b \approx 4$ Å,[14] one calculates 1.73 eV/Å for each misfit dislocation. Hence, based on our empirical results there should be about 1 dislocation for every 20 lattice planes cutting (001), i.e., a dislocation spacing of $\lambda_d=28$ Å corresponding to a density of 3.6×10^6 cm^{-1}.[52]

It is instructive to compare this estimate with the dislocation density naively obtained for a cubic misfit picture, in which the interface dislocations arise solely from the 18% volume difference between transformed (β) and untransformed (α) SL constituents. Although such a simplified picture is more suited to layer-by-layer epitaxial growth than to sudden first-order phase transitions, we use it here to establish a density minimum. Assuming that the transition misfit $q \sim (1/3)(\Delta V/V)^{\beta\alpha}$, as appropriate for the ZB→B1 structural change, one obtains a strain-relaxed (i.e., DI limit) dislocation density of $|q|/b = 1.5\times10^6$ cm^{-1}. This is about half of our empirical result. Since the different lattice structure between the β and α phases could easily account for a factor of two more dislocations, we find that the interpretation of $\sigma^{\beta\alpha}$ using Eq. (8) within the context of the DI limit gives sensible results. At present, it is not possible to say more about the nature or number of the transition-induced interface dislocations without knowing the actual crystal structure of the AlAs β phase. Careful high-pressure x-ray experiments on SL's with different layer thicknesses should be pursued in this regard.

Let us now try to establish the specific conditions under which it becomes preferable to view the stability of AlAs/GaAs SL's in terms of the EA limit. According to Fig. 3 and the discussion at the end of Sec. II, this should depend on whether the minimum nucleation size for β material within an α medium is large enough to encompass several SL periods, thereby averaging the stability of AlAs and GaAs. For each bulk constituent, Eq. (2) of Paper I provides a crude estimate of the minimum nucleation radius r^* from a knowledge of the *homointerface* energy density $\sigma_0^{\beta\alpha}$ and the transition hysteresis.[28] We shall employ the same expression here under the assumption that $\sigma_0^{\beta\alpha} \approx \sigma^{\beta\alpha}=0.12$ eV/Å^2, i.e., that the β/α homointerface energy, which produces hysteresis in bulk material, is similar to the heterointerface term causing the AlAs overpressing in SL's. This approximation is supported by the chemical similarity of AlAs and GaAs, but for heterostructure constituents differing more strongly in ionicity it will be rather less reliable. Based on the measured range of hysteresis, i.e., $P_1^t - R^t$ or $P_2^t - R^t$, which varies from 6 GPa in bulk AlAs (see Paper I) to as high as 11 GPa in the thin-layer SL's (Table I), r^* is estimated to be in the range 40–70 Å for all SL and BL samples. This would imply that SL4–SL6 could be governed by the EA limit. Since experiment does not bear this out, i.e., the thresholds are not given by Eq. (13), we find that it is probably necessary to average two or more SL periods within the minimum nucleation size before the EA limit takes over. Furthermore, in borderline cases, the shape of the β-phase nuclei will figure importantly in how many SL periods are encompassed by each nucleus. For example, a greater tendency to form lenticular [001]-oriented platelets in SL's, compared to more spherical nuclei in bulk material, could shift the onset of the EA limit to thinner layers.

Finally, consider the compatibility of the DI limit with the observed trends for increasing transition-induced disorder in thinner-layer SL's. It was found in Paper I that the average ZB micrograin *diameter* after cycling through the forward and reverse transitions is ~65 Å in bulk GaAs and ~175 Å in bulk AlAs. Given the preceding estimate of $r^* \sim 40$–70 Å, we expect that transformed-phase nuclei will not grow appreciably beyond their formation size in GaAs, but might grow to roughly twice this size in AlAs.

If the DI limit applies, this picture of nucleation and grain growth should lead to several verifiable consequences in the postreversal data of Sec. IV. When the layer thickness for both SL constituents is appreciably greater than ~175 Å, the postreversal spectra are expected to resemble those found in bulk AlAs and GaAs; interface modes that previously appeared under favorable resonance excitation should be absent or severely broadened. This is borne out for SL1 (our thickest-layer SL) in Figs. 14(b) and 14(c), compared to Fig. 14(a). SL2 and SL3 have much thinner *AlAs* layers than SL1. Accordingly, the DI model predicts that their AlAs scattering should be more sensitive to encroachment of transformed nuclei across the interfaces from the GaAs side. This effect is

absent for SL2 in Fig. 15(b) because the GaAs layers have not yet transformed. However, for SL3 [Figs. 16(c) and 16(d)], the disorder from cross-interface nucleation is evident in the single broad triangular peak between the AlAs TO(Γ) and LO(Γ) frequencies after both constituents have transformed. The insensitivity of the GaAs scattering in SL3 to this interface disorder is explained by the greater thickness of the GaAs layers (viz., $h_g/h_a=4$, Table I).

The postreversal situation for the thin-layer SL's is more complicated because r^* is now *comparable* to the layer thickness. Accordingly, the DI model suggests that cross-interface nucleation should produce *both* interface and bulklike disorder, and broadband evidence of this was presented for SL4 and SL5 [Figs. 17(c) and 10(d)–10(f)].[50] Indeed, the high-pressure β-phase spectra of SL5 exhibit considerable bulk GaAs disorder, perhaps to the point of amorphization as recently reported for decompression of bulk GaAs from *megabar* pressures.[53] The lack of a strong increase in bulk or interface disorder in the postreversal spectrum of SL6 [Fig. 11(d)] indicates little cross-interface encroachment of grain growth. This leads us to speculate that SL6 may be a case of lenticular platelet formation, promoted by the AlAs and GaAs layer thicknesses being reversed relative to SL4 and SL5. Further Raman and x-ray experiments are planned to explore the detailed nature of postreversal disorder in AlAs/GaAs SL's.[54] However, on balance we find that the DI limit provides a plausible explanation for the trends encountered so far.

VI. CONSEQUENCES

In Sec. IV E of the present paper, a summary was presented of the major experimental findings concerning pressure-induced polymorphic transitions in SL's. Here, we emphasize the physical consequences of these results, making connections to the nucleation effects discussed in Paper I, and to the stability of as-grown epitaxial structures under ambient pressure conditions.

The observed AlAs overpressing without GaAs underpressing in AlAs/GaAs SL's demonstrates that the effective stability (300 K) of these systems against high-pressure α-β phase changes is GaAs controlled over a wide range of layer thicknesses. This enhanced stability of epitaxial AlAs is attributed to heterointerface energy contributions. From the slope of P_1^t vs $1/h_a$ (in Fig. 13) we obtain the energy per unit area of a *nonpseudomorphic* sixfold-fourfold β-AlAs/α-GaAs interface, $\sigma^{\beta\alpha}=0.12\pm0.02$ eV/Å^2. Note that this central result (we have found no previous measurement for semiconductors) follows from a thermodynamic treatment of the data via Eq. (6). Hence, the obtained value of $\sigma^{\beta\alpha}$ is not model specific.

As one might expect, $\sigma^{\beta\alpha}$ is much larger than the energy per unit area of any conventional fourfold-fourfold heterointerface between chemically similar or dissimilar semiconductors. Recent microscopic calculations find that α/α interfaces typically have energy densities $\sigma^{\alpha\alpha}\sim\pm1$ meV/Å^2,[26] which, according to Eqs. (6) and (7), could contribute at most 1 GPa of overpressing or underpressing in a monolayer SL, and proportionately less for SL's with thicker layers. Hence, only for constituents such as Sn and InSb, having low bulk transition thresholds (1 bar and 2.2 GPa, respectively[3,20]), should the strain and charge-exchange contributions to $\sigma^{\alpha\alpha}$ have an appreciable effect on the high-pressure α-β transitions in SL's. From this, we believe that a wide variety of strained-layer SL's should exhibit overpressing phenomena qualitatively similar to those in AlAs/GaAs, in spite of possible large differences in lattice constant and ionicity between their constituents.

Martin[8] has addressed the issue of whether a *pseudomorphic* sixfold-fourfold AlAs/GaAs SL could be stable at high pressure, and concludes that the lowest energy pseudomorphic interfaces result from alternating sixfold fourfold stacking along [111]. The analysis in Fig. 18 suggests that such a highly strained arrangement could be favored over the DI limit for $h_a<90$ Å. However, our Raman data for SL2 and SL3 do not show a large strain in GaAs after the AlAs layers transform; rather, the observed trends point to increased interface disorder following the transitions in thinner-layer (h_a *or* h_g) SL's. Combined with the absence of GaAs underpressing, we are forced to conclude that the proper model for the SL phase transitions studied here is the DI limit.

Although the standard misfit-dislocation pictures[13,14,25] are too simple for the phase-transition problem, Eq. (8) is generic enough to yield a reasonable post-transition dislocation density $1/\lambda_d$ when fit to the AlAs overpressing. The apparent absence of a pseudomorphic sixfold-fourfold phase probably stems, in large part, from nucleation effects which are excluded from the Ref. 8 theory. These effects become important for $h_a<90$ Å since the minimum nucleation size ($2r^*\sim80$–140 Å) is of this order. Hence, the actual SL phase-transition problem is quite complicated, requiring a theoretical treatment of interacting α-β boundaries—namely, the kinetic boundaries of transformed nuclei and the static planar interfaces of SL's. However, as suggested in Paper I, a low-energy pseudomorphic (111) sixfold-fourfold *homointerface* might still be realized during the initial growth stages of β nuclei, since their formation will tend to occur by a minimum energy path.

We have argued that the EA limit should apply when two or more SL periods fit within $2r^*$. It is worth noting that this limit is alloylike only with regard to the threshold for pressure-induced SL transitions. Actual alloy formation in the β/α phase is not expected because transition-induced *chemical* mixing is unlikely to be appreciable at 300 K. This is quite different from eptiaxial growth, where chemical mixing effects in atomic-dimension SL's have been shown to compete strongly with ordered growth and disproportionation.[26]

Finally, there seems to be virtually no chance for ambient-pressure growth of a pseudomorphic sixfold-fourfold SL in any materials systems, since the interface energy would be simply too large. However, in some systems this might be used to advantage in the following way.[35] A number of rocksalt structure A_NB_{8-N} compounds (e.g., CdO, MgO, AgBr, MnSe, etc.) with ionicity greater than 0.785 are thought to "undergo" the α-β

transition at negative pressures.[55] Hence, with the right choice of ZB substrate, it might be possible to "overpress" the normally unstable ZB phase of these materials into the positive pressure regime, thereby allowing epitaxial growth of new metastable heterostructures. The well-known MnSe/ZnSe system[18] mentioned in the Introduction falls under this category. We note that several oxide candidates for such heterostructures might be of interest as insulating layers in metal-insulator-semiconductor (MIS) applications.

ACKNOWLEDGMENTS

This work was supported in part by ONR Contract No. N00014-89-J-1797, and by grants from the Xerox Webster Research Center, and the Center for Electronic and Electro-optic Materials at SUNY-Buffalo. The authors are grateful to M. Cardona for suggestions concerning the importance of nucleation, M. Holtz for helpful discussions, and R. Burnham for making available OMCVD samples. Thanks are due also to G. Orffeo of Graphtrix, Inc. for digital image processing.

---

*Present address: Department of Physics, Harvard University, Cambridge, MA 02138.

†Present address: Department of Physics, Oakland University, Rochester, MI 48309.

[1]H. G. Drickamer, in *Solid State Physics: Advances in Research and Applications,* edited by F. Seitz and D. Turnbull (Academic, New York, 1965), Vol. 17, p. 1.

[2]W. Klement and A. Jayaraman, in *Progress in Solid State Chemistry,* edited by H. Reiss (Pergamon, London, 1967), Vol. 3, p. 289.

[3]S. C. Yu, I. L. Spain, and E. F. Skelton, Solid State Commun. **25**, 49 (1978); S. C. Yu, C. Y. Liu, I. L. Spain, and E. F. Skelton, in *High Pressure Science and Technology,* edited by K. D. Timmerhaus and M. S. Barber (Plenum, New York, 1979), Vol. 1, p. 274.

[4]J. C. Phillips, Phys. Rev. Lett. **27**, 1197 (1971); J. A. Van Vechten, Phys. Rev. B **7**, 1479 (1973).

[5]M. T. Yin and M. L. Cohen, Phys. Rev. Lett. **50**, 1172 (1983); **50**, 2006 (1983).

[6]R. Biswas, R. M. Martin, R. J. Needs, and O. H. Nielsen, Phys. Rev. B **30**, 3210 (1984); **35**, 9559 (1987); K. Kunc and R. M. Martin, *ibid.* **24**, 2311 (1981).

[7]B. A. Weinstein, S. K. Hark, R. D. Burnham, and R. M. Martin, Phys. Rev. Lett. **58**, 781 (1987); B. A. Weinstein, S. K. Hark, and R. D. Burnham, in *The Physics of Semiconductors,* edited by O. Engström (World Scientific, Singapore, 1987), Vol. 1, p. 707.

[8]R. M. Martin, in *The Physics of Semiconductors,* edited by O. Engström (World Scientific, Singapore, 1987), Vol. 1, p. 639.

[9]B. A. Weinstein, Semicond. Sci. Technol. **4**, 283 (1989).

[10]L. J. Cui, U. D. Venkateswaran, B. A. Weinstein, and F. A. Chambers, in *The Physics of Semiconductors,* edited by E. Anastassakis and J. D. Joannopoulos (World Scientific, Singapore, 1991), Vol. 2, p. 953.

[11]See, for example, *Epitaxial Growth,* edited by J. W. Matthews (Academic, New York, 1975), especially Chaps. 1, 2, and 9; *Applications of Multiquantum Wells, Selective Doping, and Superlattices,* Vol. 24 of *Semiconductors and Semimetals,* edited by R. Dingle (Academic, New York, 1987).

[12]L. L. Chang, J. Vac. Sci. Technol. B **1**, 120 (1983).

[13]J. H. Van der Merwe, in *Single Crystal Films,* edited by M. H. Francombe and H. Sato (Pergamon, New York, 1964), p. 139; J. H. Van der Merwe, J. Woltersdorf, and W. A. Jesser, Materials Sci. Eng. **81**, 1 (1986), and references therein.

[14]J. W. Matthews, J. Vac. Sci. Technol. **12**, 126 (1975); J. W. Matthews and A. E. Blakeslee, J. Cryst. Growth **27**, 118 (1974); **29**, 273 (1975); J. W. Matthews, A. E. Blakeslee, and S. Mader, Thin Solid Films **33**, 253 (1976).

[15]A. A. Mbaye, D. M. Wood, and A. Zunger, Phys Rev. B **37**, 3008 (1988); D. M. Wood and A. Zunger, Phys. Rev. Lett. **61**, 1501 (1988).

[16]C. G. Van de Walle and R. M. Martin, Phys. Rev. B **34**, 5621 (1986).

[17]G. A. Prinz, Phys. Rev. Lett. **54**, 1051 (1985).

[18]L. A. Kolodziejski, R. L. Gunshor, N. Otsuka, B. P. Gu, Y. Hefetz, and A. V. Nurmiko, Appl. Phys. Lett. **48**, 1482 (1986).

[19]B. T. Jonker, J. J. Krebs, S. B. Qadri, G. A. Prinz, F. Volkening, and N. C. Koon, J. Appl. Phys. **63**, 3303 (1988).

[20]R. F. C. Farrow, D. S. Robertson, G. M. Williams, A. G. Cullis, G. R. Jones, I. M. Young, and P. N. J. Dennis, J. Cryst. Growth **54**, 507 (1981); J. Menendez and H. Höchst, Thin Solid Films **111**, 375 (1984).

[21]The term "superpressed" used in the earlier work is replaced here by "overpressed." This usage is more appropriate, since the observed stability modifications are essentially static effects due to the presence in SL's of *fixed* heterointerfaces.

[22]B. A. Weinstein, in *The Proceedings of the SPIE Conference on Quantum Well and Superlattice Physics,* edited by G. Döhler and J. Schulman (SPIE, Washington, 1987), Vol. 792, p. 66.

[23]M. Holtz, K. Syassen, and K. Ploog, Phys. Rev. B **40**, 2988 (1989).

[24]B. Gil and D. J. Dunstan, Semicond. Sci. Technol. **6**, 428 (1991).

[25]R. People and S. A. Jackson, in *Strained Layer Superlattices: Physics,* Vol. 32 of *Semiconductors and Semimetals,* edited by T. P. Pearsall (Academic, New York, 1990), Chap. 4; R. People and J. C. Bean, Appl. Phys. Lett. **47**, 322 (1985).

[26]R. G. Dandrea, J. E. Bernard, S.-H. Wei, and A. Zunger, Phys. Rev. Lett. **64**, 36 (1990); S.-H. Wei and A. Zunger, *ibid.* **61**, 1505 (1988); D. M. Wood, S.-H. Wei, and A. Zunger, Phys. Rev. B **37**, 1342 (1988).

[27]N. A. Jesser, Mater. Sci. Eng. **4**, 279 (1969).

[28]R. E. Hanneman, M. D. Banus, and H. C. Gatos, J. Phys. Chem. Solids **25**, 293 (1964).

[29]F. P. Bundy, J. Chem. Phys. **41**, 3809 (1964).

[30]In the present work, the elastic constants for bulk AlAs and GaAs are taken from S. Adachi, J. Appl. Phys. **58**, R1 (1985).

[31]L. D. Landau and E. M. Lifshitz, *Theory of Elasticity* (Pergamon, New York, 1984).

[32]J. W. Matthews and A. E. Blakeslee, J. Cryst. Growth **32**, 265 (1976).

[33]J. C. Jamieson, Science **139**, 762 (1963); **139**, 845 (1963).

[34]F. R. N. Nabarro, *Theory of Crystal Dislocations* (Dover, New York, 1967), p. 75.

[35]S. Froyen, S.-H. Wei, and A. Zunger, Phys. Rev. B **38**, 10 124 (1988).

[36]S. Froyen and M. L. Cohen, Phys. Rev. B **28**, 3258 (1983).

[37]P. M. Raccah, J. W. Garland, Z. Zhang, F. A. Chambers, and

D. J. Vezzetti, Phys. Rev. B **36**, 4271 (1987); I. K. Schuller, M. Grimsditch, F. Chambers, G. Devane, H. Vanderstraeten, D. Neerinck, J.-P. Locquet, and Y. Bruynseraede, Phys. Rev. Lett. **65**, 1235 (1990).

[38]R. D. Burnham, D. R. Scifres, and W. Streifer, Appl. Phys. Lett. **41**, 228 (1982).

[39]C. Colvard, T. A. Gant, M. V. Klein, R. Merlin, R. Fischer, H. Morkoç, and A. C. Gossard, Phys. Rev. B **31**, 2080 (1985); M. V. Klein, IEEE J. Quantum Electron. **QE-22**, 1760 (1986).

[40]R. A. Logan and F. K. Reinhart, J. Appl. Phys. **44**, 4172 (1973).

[41]L. J. Cui, U. D. Venkateswaran, B. A. Weinstein, and F. A. Chambers, Semicond. Sci. Technol. **6**, 469 (1991).

[42]G. J. Piermarini and S. Block, Rev. Sci. Instrum. **46**, 973 (1975).

[43]P. Seguy, J. C. Maan, G. Martinez, and K. Ploog, Phys. Rev. B **40**, 8452 (1989).

[44]M. Holtz, U. D. Venkateswaran, K. Syassen, and K. Ploog, Phys. Rev. B **39**, 8458 (1989).

[45]See, for example, B. Jusserand and M. Cardona, in *Light Scattering in Solids V,* edited by M. Cardona and G. Güntherodt, Topics in Applied Physics Vol. 66 (Springer, Berlin, 1989), Chap. 3; A. K. Sood, J. Menendez, M. Cardona, and K. Ploog, Phys. Rev. Lett. **54**, 2115 (1985).

[46]R. Zallen, M. Holtz, A. E. Geissberger, R. A. Sadler, W. Paul, and M-L. Théye, J. Noncryst. Solids **114**, 795 (1989).

[47]U. D. Venkateswaran, L. J. Cui, B. A. Weinstein, and F. A. Chambers, Phys. Rev. B **43**, 1875 (1991).

[48]A. Jayaraman, in *Synthesis and Properties of Metastable Phases,* edited by E. S. Machlin and T. J. Rowland (The Metallurgical Society of AIME, Pittsburgh, 1980), p. 75.

[49]In Paper I we estimate, based on achieving transparency for the given thicknesses of BL1 and BL2, that the reversed fractions in AlAs and GaAs approach ~90%.

[50]Similar broadbands were also noted (without giving spectra) in Ref. 23 during pressure studies of very thin layer GaAs/AlAs SL's; M. Holtz (private communication).

[51]W. T. Read and W. Shockley, Phys. Rev. **78**, 275 (1950).

[52]If, as suggested in Ref. 25, screw dislocations are favored over the edge variety described by Eq. (8), the dislocation density would increase by a factor of 1.4. More realistically, the actual situation corresponding to the DI limit probably involves a wide distribution of different dislocation types.

[53]Y. K. Vohra, H. Xia, and A. L. Ruoff, Appl. Phys. Lett. **57**, 2666 (1990).

[54]U. D. Venkateswaran, D. J. Thiel, K. E. Brister, B. A. Weinstein, and D. H. Bilderback (unpublished).

[55]A. Navrotsky and J. C. Phillips, Phys. Rev. B **11**, 1583 (1975).

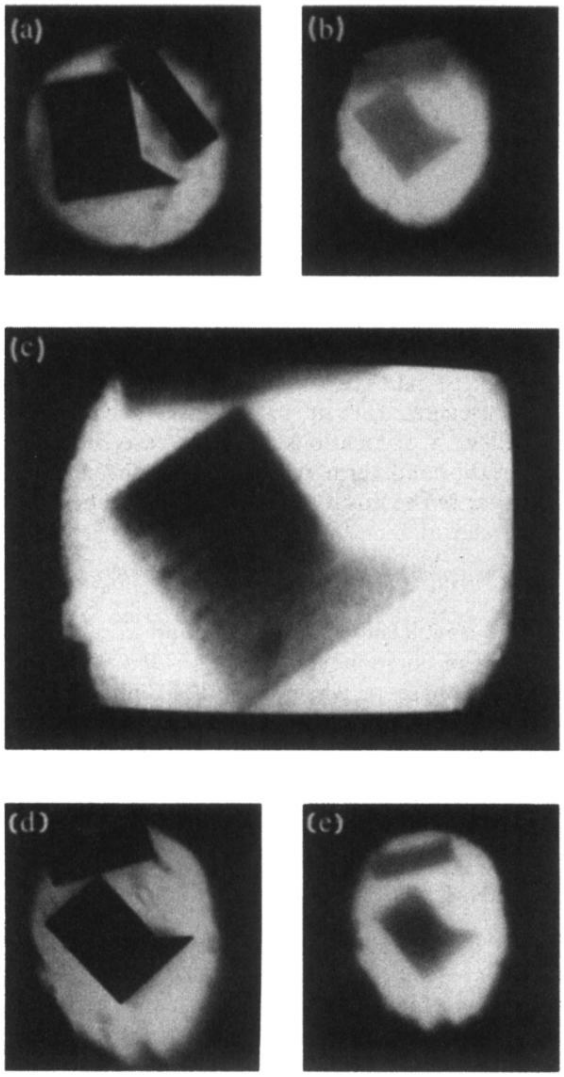

FIG. 1. Photomicrographs showing free-standing specimens of SL2 (GaAs/AlAs 225 Å/75 Å, see Table I) undergoing high-pressure phase transitions in the DAC. (a) 0.3 GPa. Initial state of sample is visibly opaque. (b) 10.5 GPa. Band gap has increased to ~ 2.3 eV. (c) 14.6 GPa at AlAs transition. Sample is held in partly transformed state—opaque region contains β-AlAs/α-GaAs. (d) 16.5 GPa. AlAs transition is complete; GaAs is still in ZB (α) phase. (e) 8.5 GPa on first cycle down of pressure. Most [$\sim 90\%$, note cloudiness compared to (b)] of β-AlAs has reversed to ZB phase; see text. Frames were digitized from color super-VHS tape for processing and printing.